The relationship between eruptive activity, flank collapse and sea-level at volcanic islands: a long-term (>1 Ma) record offshore Montserrat, Lesser Antilles

Maya Coussens

School of Ocean and Earth Science, National Oceanography Centre, University of Southampton, European Way, Southampton, SO14 3ZH, UK (mfc1e12@soton.ac.uk)

Deborah Wall-Palmer

School of Geography, Earth and Environmental Sciences, Plymouth University, Plymouth PL4 8AA, UK (deborah.wall-palmer@plymouth.ac.uk)

Peter. J. Talling

National Oceanography Centre, Southampton, Southampton S014 3ZH, UK (peter.talling@noc.ac.uk)

Sebastian. F. L. Watt

School of Geography, Earth and Environmental Sciences, University of Birmingham, Edgbaston, Birmingham, B15 2TT, UK (s.watt@bham.ac.uk)

Michael Cassidy

Institute of Geosciences, Johannes Gutenberg, University Mainz, J- J- Becher- Weg 21, D-55128, Mainz, Germany (mcassidy@uni-mainz.de)

Martin Jutzeler

National Oceanography Centre, Southampton, University of Southampton, Southampton S014 3ZH, UK (jutzeler@gmail.com)

Michael. A. Clare[1], James. E. Hunt[2]

National Oceanography Centre, Southampton, Southampton S014 3ZH, UK (michael.clare@noc.ac.uk)[1], (James.Hunt@noc.ac.uk)[2]

Michael Manga

Department of Earth & Planetary, Science University of California, Berkeley, 307 McCone Hall, Berkeley, CA, 94720, USA (manga@seismo.berkeley.edu)

Thomas. M. Gernon[1], Martin. R. Palmer[2], Stuart. J. Hatter[3]

School of Ocean and Earth Science, National Oceanography Centre, University of Southampton, European Way, Southampton, SO14 3ZH, UK (Thomas.Gernon@noc.soton.ac.uk)[1], (m.palmer@noc.soton.ac.uk)[2], (sjh1e13@soton.ac.uk)[3]

Georges Boudon

Équipe de Géologie des Systèmes Volcaniques, Institut de Physique du Globe de Paris, Sorbonne, Paris Cité, UMR 7154 CNRS, 1 Rue Jussieu Paris, 75238, France (boudon@ipgp.fr)

Daisuke Endo

Earth Evolution Sciences, University of Tsukuba, Tennodai 1-1-1, Tsukuba, Ibaraki, 305-8572, Japan (daisuke.endo.000@gmail.com)

Akihiko Fujinawa
Research Institute for Natural Hazards and Disaster Recovery, Niigata University, Ikarashi 2-8050, Nishi-ku, Niigata, 950-2181, Japan (fujinawa.INET.TheWorld@iodp.tamu.edu)

Robert Hatfield
9 College of Oceanic and Atmospheric Sciences, Oregon State University, 104 COAS Administration Building, Corvalis, OR 97331-5503, USA (rhatfield@coas.oregonstate.edu)

Matthew. J. Hornbach
Institute for Geophysics, University of Texas at Austin, J.J. Pickle Research Campus, Building 196, 10100, Burnet Road, Austin, TX, 78758-4445, USA (matt.hornbach@gmail.com)

Osamu Ishizuka
Geological Survey of Japan (AIST), Central 7, Higashi 1-1-1, Tsukuba, Ibaraki, 305-8567, Japan (o-ishizuka@aist.go.jp)

Kyoko Kataoka
Research Institute for Natural Hazards and Disaster Recovery, Niigata University, Ikarashi 2-8050, Nishi-ku, Niigata, 950-2181, Japan (kataoka@gs.niigata-u.ac.jp)

Anne Le Friant

Équipe de Géologie des Systèmes Volcaniques, Institut de Physique du Globe de Paris, Sorbonne, Paris Cité, UMR 7154 CNRS, 1 Rue Jussieu Paris, 75238, France (lefriant@ipgp.fr)

Fukashi Maeno

Earthquake Research Institute, University of Tokyo, 1-1-1 Yayoi, Bunkyo-ku, Tokyo, 113-0032, Japan (fmaeno@eri.u-tokyo.ac.jp)

Molly McCanta

Department of Geology, Tufts University, 2 North Hill Road, Lane Hall Medford, MA 02155, USA (molly.mccanta@tufts.edu)

Adam. J. Stinton

Montserrat Volcano Observatory, Flemmings, Montserrat (adam@mvo.ms)

Seismic Research Center, University of the West Indies, St. Augustine, Trinidad and Tobago

Key Points

Heightened volcanic activity on Montserrat at 120-190 ka, 760-810 ka, and 900-930 ka

Large landslides coincide with rapid sea-level rise at island arc volcanoes

Abstract

Hole U1395B, drilled southeast of Montserrat during Integrated Ocean Drilling Program Expedition 340, provides a long (>1 Ma) and detailed record of eruptive and mass-wasting events (>130 discrete events). This record can be used to explore the temporal evolution in volcanic activity and landslides at an arc volcano. Analysis of tephra fall and volcaniclastic turbidite deposits in the drill cores reveals three heightened periods of volcanic activity on the island of Montserrat (~930 ka to ~900 ka, ~810 ka to ~760 ka, and ~190 ka to ~120 ka) that coincide with periods of increased volcano instability and mass-wasting. The youngest of these periods marks the peak in activity at the Soufrière Hills volcano. The largest flank collapse of this volcano (~130 ka) occurred towards the end of this period, and two younger landslides also occurred during a period of relatively elevated volcanism. These three landslides represent the only large (>0.3 km^3) flank collapses of the Soufrière Hills edifice, and their timing also coincides with periods of rapid sea-level rise (>5 m/ka). Available age data from other island arc volcanoes suggests a general correlation between the timing of large landslides and periods of rapid sea-level rise, but this is not observed for volcanoes in intra-plate ocean settings. We thus infer that rapid sea-level rise may modulate the timing of collapse at island arc volcanoes, but not in larger ocean-island settings.

Key words

Landslide, volcanism, sea-level, IODP, Expedition 340

1. Introduction

Volcanic islands in arc settings grow and decay through eruptive and mass-wasting processes. The rate of island growth reflects the balance of these processes, including the style, composition and magnitude of individual eruptions [Houghton et al., 1995; Singer et al., 2008; Germa et al., 2010], and variations in the magnitude and frequency of mass-wasting events (e.g. lava dome collapses, flank landslides) [Ablay and Marti, 2000; Cole et al., 2002; Trofimovs et al., 2013]. As a volcanic island grows, the edifice becomes increasingly unstable, resulting in partial flank collapses, which are a ubiquitous feature of composite volcanoes (e.g. Siebert, 1984). Such collapse events are potential geohazards through the generation of landslides [Siebert, 1984; Watt, et al., 2012a, 2012b], and their potential to generate tsunamis [Ward and Day, 2003]. There are few individual volcanic records that span the life cycle of individual composite volcanoes (on the order of 10^5 to 10^6 years), but such records can be used to investigate temporal patterns in total volcanic output, and the relative timing of flank collapses. The instabilities that drive collapses may relate both to internal (e.g. total volcanic output) and external (e.g. eustatic sea-level change) processes. To obtain a more complete understanding of the overall controls on volcano growth and destruction, we use a marine stratigraphic record offshore Montserrat to explore patterns of volcanism, sea-level change and flank collapse timing over a 10^6 year period.

Here, we use the term flank collapse to refer to gravity-driven failures of volcanic material from subaerial and/or submarine volcanic island flanks, potentially also involving carbonate shelf material. Collapses that only involve material from the carbonate shelf (i.e. generating bioclastic deposits) are referred to as shelf collapses. Flank collapses can involve several cubic kilometres of material, and may or may not be associated with volcanic eruptions. They are distinct from the generally smaller dome collapses, which involve juvenile lava and are a common mass wasting process during the lava-dome forming eruptions that typify volcanism on Montserrat. *Mass-wasting* or *landslides* are used as collective terms here for the different types of collapse events. Landslides may also generate a range of density currents that are represented in the geological record as a variety of density current deposits. In this study we refer to all submarine density current deposits as *turbidites*, regardless of whether the deposits were generated from fully turbulent or non-turbulent flows.

Triggers of flank or shelf collapses on volcanic islands are poorly understood, but it has been proposed that their frequency is related to eustatic sea-level changes, edifice growth, tectonic activity, and rainfall [McGuire et al., 1997; Masson et al., 2006; Sato et al., 2007; Marques et al., 2008; Quidelleur et al., 2008; Hunt et al., 2013, 2014]. Reconstructing pre-historical earthquake and rainfall records are challenging, resulting in difficulties when comparing these potential triggers to landslide occurrence. Previous studies of eustatic sea-level change and landslides have been hampered due to difficulties in acquiring sufficient and accurate dates for landslide events. Such studies have typically relied on incomplete information from on-land observations of collapse structures, and/or been restricted to relatively recent events recorded in shallow (<6 m) marine sediment cores and seismic profiles [McMurtry et al., 2004a, 2004b; Boudon et al., 2007; Trofimovs et al., 2013]. Consequently, very few volcanic island landslide events have been dated precisely over time periods that are long enough to include multiple climatic, volcanic, and tectonic cycles [Longpré et al., 2011; Trofimovs et al., 2013; Hunt et al., 2013].

We analysed Hole U1395B from IODP Expedition 340, drilled in 2012. This Hole is >120 m in length and contains an unusually long (>1 Ma) and detailed marine record of island arc volcanism and mass-wasting activity. Hole U1395B was drilled ~25 km southeast of Montserrat at ~1200 m below sea-level (Figure 1), and provides an excellent opportunity to study a long and detailed record of sedimentological processes around an island arc volcano.

The record of marine volcaniclastic deposits (both turbidites and tephra fall deposits) is used as a proxy for volcanic activity at Montserrat. This approach is based on studies of marine deposits associated with the 1995-2010 eruption on Montserrat [Kokelaar, 2002; Trofimovs et al., 2006], which showed that individual pyroclastic flows formed via dome-collapse and explosive eruption events produced widespread volcaniclastic turbidites. We thus expect most volcaniclastic turbidites to represent individual eruptions, but note that some volcaniclastic turbidites may be produced by non-eruptive flank collapses, or by reworking of older volcaniclastic deposits. Turbidites from large flank collapses can be identified by their thickness and correlation with debris avalanche deposits (and there are only a few of these around Montserrat; cf. Lebas et al., 2011), while resedimented turbidites may be more mixed, including bioclastic material. The latter may also still provide a broad proxy for volcanic activity, since they are more likely to be generated during periods of volcanism, when flanks may be destabilised by eruptive activity and deposition of volcanic products [Collins and Dune et al., 1986; Major et al., 2000; Hunt et al., 2014].

By identifying and dating volcaniclastic deposits from Hole U1395B, we aim to investigate the temporal relationships between mass-wasting, volcanic activity, and sea-level over an interval of ~10^6 years. This period encompasses a sufficient number of volcanic cycles and eustatic sea-level changes to allow for statistically robust hypothesis testing. It is also shown that all of the well-dated major collapse events around Montserrat occurred during periods of rapid sea-level rise. We explore whether other volcanic islands (island arcs and intraplate ocean islands) show similar relationships between landslide ages and sea level or volcanism, whilst noting that many of these landslide ages have considerable uncertainties.

2. Study Area: Introduction to Montserrat

Montserrat is an island arc volcano located in the Lesser Antilles (Figure 1), which erupted between 1995-2010, devastating the city of Plymouth and affecting large parts of the island economy [Kokelaar et al., 2002; Wadge et al., 2014]. The eruptions included collapse of the active lava dome generating pyroclastic flows and block and ash flows. The largest dome collapse (0.21 km^3) occurred in 2003 and generated a 0.5-1 m high tsunami on Guadeloupe [Herd et al., 2006; Trofimovs et al., 2008]. Bathymetric mapping has since identified much larger landslide deposits offshore Montserrat with volumes of 0.3-20 km^3 [Deplus et al., 2001; Boudon et al., 2007; Lebas et al., 2011; Watt et al., 2012a, 2012b]. Such large landslides have a much higher tsunamigenic potential, and thus represent a more significant hazard than events associated with the recent eruptions.

Since ~290 ka (based on subaerial Ar-Ar dates; Harford et al., [2002]), activity at Montserrat has been focussed on the andesitic Soufrière Hills volcano, except for a brief interlude of basaltic volcanism at ~130 ka, forming the South Soufrière Hills (Figure 1). The previously active volcanic centre, at Centre Hills, is dated at 990-550 ka [Harford et al., 2002]. Between these two periods of activity (550 ka to 290 ka) the subaerial record suggests a period of quiescence. The apparent gap in volcanism from 550 ka to 290 ka is not clear in the marine sediment cores, and the existing subaerial ages may thus reflect a limited stratigraphy represented by on-land exposures, or incomplete study and dating of subaerial outcrops.

The offshore eruption and landslide record around Montserrat has been studied in detail [Deplus et al., 2001; Trofimovs et al., 2006, 2010, 2012, 2013; Boudon et al., 2007; Lebas et al., 2011; Le Friant et al., 2010, 2015; Cassidy et al., 2012b, 2013]. To the southeast and southwest of Montserrat is an extensive shallow core (<6 m) data set (Figure 1). These >80 cores contain hemipelagic sediment and numerous volcaniclastic and bioclastic turbidites from eruption and landslide deposits emplaced during the last ~110 ka [Le Friant et al., 2009; Trofimovs et al., 2010, 2012, 2013; Cassidy et al., 2012b, 2013]. Swath bathymetry and 2D and 3D seismic data reveal seven large landslide deposits, dating back to the time of Centre Hills volcanism (Figure 1). These large landslide deposits likely represent flank collapse events as opposed to dome or localised shelf collapses.

It is important to recognise that any study based on a single sampling site will introduce some sampling bias in the record of eruptive and collapse events. The activity at Montserrat is typified by dome-forming eruptions with durations of months to years, interspersed by moderate-sized explosive pulses such as the 1995-2010 eruption [Kokelaar, 2002; Wadge et al., 2014]. Such eruptions form complex volcaniclastic intervals generated by multiple pyroclastic density currents and tephra fall events distributed radially from the volcanic edifice [Trofimovs et al., 2006, 2013; Le Friant et al., 2015]. Hole U1395B is located ~25 km southeast of Montserrat, hence it is only likely to sample mass flows that entered the ocean to the east and south of Montserrat. While some individual events may therefore not be preserved within Hole U1395B, periods of eruption are still likely to be represented, because any one eruption is likely to produce multiple mass flow and tephra fall deposits, with the mass flows, in particular, travelling in a range of directions. For example, the 2003 collapse event (0.1 km^3) deposited a ~20 cm thick volcaniclastic turbidite at site U1395B [Trofimovs et al., 2008], but small vulcanian eruptions that occurred throughout the 1995-2010 eruption are not represented within Hole U1395B [Kokelaar, 2002; Wadge et al., 2014].

Hole U1395B is only likely to sample a small proportion of tephra fall deposits, as dispersal depends on wind direction and the magnitude of the explosive event. Prevailing wind directions in the troposphere and upper stratosphere are predominantly from the east, and prevailing wind directions in the lower stratosphere are from the west, based on historical data from 1956 to present [Radiosonde wind dataset on Guadeloupe]. Tephra fall deposits may therefore be subject to a spatial sampling bias, with many eruption plumes transported to the west leaving no record within U1395B. However, large explosive eruptions, which can involve multiple phases and be associated with pyroclastic density currents and the generation of offshore turbidites, are still likely to have some representation at the core site as an eruptive event. Because we are interested simply in event timing, rather than magnitude or style, this single core is likely to provide a relatively comprehensive record of eruptions at Montserrat.

3. Methods

3.1. Event deposit identification

We defined five facies at Site U1395: hemipelagic mud, bioclastic turbidites, mixed bioclastic-volcaniclastic turbidites, volcaniclastic turbidites, and tephra fall deposits (Figure 2). Hemipelagic mud is mostly composed of carbonate and detrital clay with abundant interspersed foraminifera. The volcaniclastic turbidite and tephra fall deposits are less easily distinguished from each other, as both can comprise normally-graded sand and silt [Trofimovs et al., 2013]. Their discrimination requires grain size and component analysis to identify the type of event deposit [Cassidy et al., 2014, 2015].

Tephra fall layers were defined in this study as having <30% bioclasts, a Folk and Ward [1957] sorting coefficient of <0.5 phi (where grainsize (phi) = - $\log_2$(grainsize (mm)) (analyses conducted on particles from -1 to 9 phi), and a thickness of <20 cm. Tephra fall deposits are well sorted by density and dominated by volcanic clasts. Hole U1395B is ~25 km away from Montserrat, where tephra fall deposits from moderate-sized explosive eruptions, even downwind, are likely to be a few centimetres thick; consequently, thick (>20 cm) deposits are unlikely to represent tephra fall layers. Large magnitude eruptions are rare within the Lesser Antilles [Palmer et al., 2016]. Thin tephra fall layers are commonly mixed with surrounding hemipelagic material, through bioturbation, bottom current reworking, or disturbance during coring, thus artificially increasing their apparent bioclast content. We thus examined the core for any evidence of post-depositional processes (Supplementary figure S1) and have defined tephra fall layers as comprising < 30% bioclast content to allow for post-depositional mixing. Volcaniclastic turbidites are deposits from high-energy, erosive flows that may entrain bioclastic material and pre-existing volcaniclastic sediments. Therefore, although some parts of a volcaniclastic turbidite can be well-sorted, they are likely to be less well-sorted than tephra fall deposits [Cassidy et al., 2014]. Volcaniclastic turbidites are defined here as comprising <30%

bioclasts, with a Folk and Ward [1957] sorting coefficient >0.5 (phi). Mixed turbidites are defined as having 30-70% bioclasts. Bioclastic turbidites are defined as containing >70% bioclasts (see Supplementary Figures S1-S3).

Grain size measurements using laser-diffraction analyses were carried out using a Malvern Master-sizer 2000 particle size analyser, which can measure grain sizes between 0.2−2000 μm. To disperse grains, 25 ml of reverse osmosis water with 0.05% sodium hexametaphosphate dispersant was added to 1 cm^3 of sample and left overnight on a shaking table. Samples were analysed in triplicate and accuracy was monitored using standard size particles (32 and 125 μm) (see Hunt et al., [2013] for details). Componentry analysis was conducted on sieved fractions >63 μm and <250 μm material from all volcanic-rich units and some bioclastic-rich units. For each sample, approximately 400 grains were point-counted using an area counting method. Componentry classes follow Le Friant et al., [2008] and Cassidy et al., [2014]: 1) vesicular pumice clasts; 2) non-vesicular andesite; 3) altered lithic clasts; 4) crystal and glass fragments; 5) mafic scoria clasts; and 6) bioclasts. Grainsize and componentry data are summarized in Table S1 and Table S2, respectively (see Supplementary Figures S1-S3 for photos).

3.2. Dating Hole U1395B

The core from U1395B core was dated using a combination of oxygen isotope stratigraphy, biostratigraphy, AMS radiocarbon dating, and the shipboard paleomagnetic reversal records. Higher resolution dating was carried out on the upper 40 m of Hole U1395B using oxygen isotope stratigraphy of the hemipelagic mud (Figure 2). Twenty *Globigerinoides ruber* specimens between 250-355 μm in size were picked and analysed from each hemipelagic sample. Samples were 7 cm apart and analysed at Plymouth

University on an Isoprime Instruments continuous flow mass spectrometer with a Gilson Multiflow carbonate auto-sampler. Oxygen Isotope values are given as deviations in the isotope ratios ($^{18}O/^{16}O$) per mil (‰), using the VPDB scale (Table S3).

To limit the ambiguity of identifying marine isotope stages, biostratigraphic boundaries and AMS radiocarbon dates (for sediments <50 ka) were used (Table 1). Calcareous nannofossils in the <63 μm material from hemipelagic samples were analysed using scanning electron microscopy (SEM), employing the calcareous nannofossil zonation of Kameo and Bralower [2000] for the Caribbean Sea. Sediment was fixed to metal stubs using a thin layer of spray adhesive, then sputter-coated with gold. The first occurrence of *Emiliania huxleyi* (250 ka) was found at 36.74 m, close to the MIS 7/8 boundary (243 ka). The first occurrence of *E. huxleyi* has also been identified across the MIS 7/8 transition in Hole U1396C [Wall-Palmer et al., 2014] and CAR-MON 2 [Le Friant et al., 2008] (Figure 3).

New AMS dates were obtained in this study from four samples in the upper 4 m of Hole U1395B (aged <57 ka), in addition to the radiocarbon AMS dates reported by Trofimovs et al., [2013]. Approximately 1000 pristine tests of white *Globgerinoides ruber* >150 μm in size were picked (~17 mg) and then sonically cleaned. The new samples were located beneath two of the largest turbidites (Figure 3). Radiocarbon dates were measured at Scottish Universities Environmental Research Council (SUERC) using their in-house protocol [see Trofimovs et al., 2013].

Paleomagnetic reversals were determined on board during Expedition 340 as 180° changes in declination (after azimuthal correction). Associated changes in inclination after demagnetization of the natural remnant magnetization (NRM) in a field of 20 mT (to remove the coring overprint) were also recorded (see Hatfield et al., [2013] for details). Here we report ages based on the geomagnetic polarity timescale (GPTS) of Ogg et al., [2012] instead of the GPTS of Cande and Kent [1995] as was reported on board the ship. Two paleomagnetic reversals occur at 781 ka (6.3% error) and 988 ka (11.3% error) in core U1395B [Cande and Kent 1992a, 1992b; Ogg et al., 2012], with a possible third reversal at the base of the core at 1072 ka (11.3% error) [Cande and Kent 1992; Ogg et al., 2012]. The 781 ka reversal is obscured by a volcaniclastic turbidite and coring disturbance at 68.5-71 m (Figure 2). The coring disturbance occurs primarily within the volcaniclastic turbidite. The reversal is likely to have occurred shortly prior to the emplacement of the volcaniclastic turbidite, thus obscuring the reversal through erosion of hemipleagic mud. Here we take the base of the volcaniclastic turbidite as 781 ka. The MIS 8/9 (300 ka) boundary is interpreted to occur at ~44 m, suggesting that sedimentation rates decrease with depth in the core. The 988 ka reversal occurred between 88.3-89.9m with a mid-point at 89.1 m (Figure 2). The 1072 ka reversal may be present at the base of Hole U1395B (Figure 2) but this is less certain due to poor sample recovery at the base of the core.

Data from Hole U1395B were also compared and correlated to previously studied cores around Montserrat (Figure 3). These cores include JR123-5V, JR123- 6V, CAR-MON 2, and Hole U1396C (Figure 3). JR123-5V and JR123-6V are part of an extensive vibrocore data set that has been used to compile a comprehensive stratigraphy of Montserrat over the past 110 ka [Trofimovs et al., 2013]. The vibrocore data set includes over 80 <6 m long cores with 40 accelerator mass spectrometry (AMS) radiocarbon dates (Figure 3). JR123-5V and JR123-6V are located 1-2 km north of Site U1395, and some units within core U1395B can be correlated to units found in JR123-5V and JR123-6V by age (Figure 3). CAR-MON 2 is a piston core collected in 2002, which extends 5.75 m and was taken ~55 km to the southwest of Montserrat (Figure 3) [Le Friant et al., 2008]. Site U1396C is situated ~33 km southwest of Montserrat (Figure 3) and was collected during IODP Expedition 340 [Wall-Palmer et al., 2014].

4. Results

Hole U1395B is 127.51 m long and it is composed of 62.6% hemipelagic mud, 24.4% volcaniclastic deposits, 9% mixed turbidites and 4% bioclastic deposits, by deposit thickness. The core comprises 18 bioclastic turbidites, 48 tephra fall deposits, 26 mixed turbidites, and 41 volcaniclastic turbidites. Core recovery is good (>90%), with only one occurrence of basal flow-in coring disturbance over the studied core length at the bottom of Core U1395B-2H, followed by probable fall-in at the top of Core Section U1395B-3H [Jutzeler et al., 2014].

4.1. Age Models

Unit ages have been estimated by calculating hemipelagic sedimentation rates between dated horizons, assuming constant sedimentation rates between dated horizons. Devoloping accurate age models for marine cores is difficult due to the effects of erosion (commonly at the base of turbidites), short-term fluctuations in sediment supply, and the sometimes ambiguous identification of marine isotope stages. We therefore include three age models to help capture these uncertainties, and their implications.

Age models can be affected by erosion. In the upper 5 m of U1395B ~88 cm of hemipelagic sediment may have been eroded by the 12-14 ka turbidite [Trofimovs et al., 2013], indicating that the effects of erosion at Site U1395B may be significant. Erosion rates in the upper 10 m of U1395B are well constrained by a combination of AMS dates from this study, and correlation with well-dated units (40 AMS dates) in the shallow vibrocore dataset [Trofimovs et al., 2013]. Below the threshold for AMS radiocarbon dating (>10 m in Hole U1395B) the effects of erosion by turbidites cannot be accurately constrained at site U1395B, potentially leading to inaccuracies in age models. It is likely that most turbidity currents are erosive, removing underlying hemipelagic mud and event deposits from the stratigraphy resulting in the underestimation of the true sedimentation rate. We expect this to be a systematic error affecting the whole core, however, rather than something that introduces bias to specific time periods.

Dating cores using oxygen isotopes may also lead to age model inaccuracies due to difficulties in identifying marine isotope stages (MIS). Oxygen isotopes from Hole U1395B have been compared to the Lisiecki and Raymo, [2005] curve; but, local factors may affect the magnitude of isotope fluctuations and erosion may remove parts of the isotope record, resulting in the misidentification of MIS boundaries. Any inaccuracies in the age models used will affect the reliability of unit ages assigned to individual events, and thus affect subsequent analysis of the dataset.

Assuming that the average total erosion beneath turbidites is on the order of centimetres, and assuming that MIS boundaries have been correctly constrained within a few centimetres, the event dating errors are likely to be on the order of 10^2-10^5 years. This is of a similar magnitude to stratigraphic gaps identified in other cores around Montserrat, including instances where >30 ka of stratigraphy was removed by turbidite erosion (JR 123-5-V and Hole U1396C) (Trofimovs et al., 2013; Wall-Palmer et al., 2014). In order to assess how sensitive our event-frequency analysis is to dating errors of this magnitude, we conduct the same analysis with three different age models. Age Model 1, described below, uses all age constraints (i.e. MIS boundaries, palaeomagnetic reversals etc.) but is also potentially more susceptible to the effects of erosion, producing a record with apparent fluctuations in sedimentation rate. Age Models 2 and 3 use fewer age constraints, resulting in a smoother estimate of long-term sedimentation rate that may be more geologically realistic. Individual unit ages derived from the three age models may vary by up to 10^5 years. By using all three age models within subsequent analyses, we can test how robust our results are to these uncertainties.

Age Model 1: This model uses 11 dated horizons, including horizons derived from correlations to units described in Trofimovs et al. [2013], identification of MIS boundaries, and identification of paleomagnetic reversals. The 2-1.5 ka, 6 ka, 14 ka, 74-59 ka, 110-103 ka, and 130 ka deposits from Trofimovs et al. [2013] and Cassidy et al. [2013] have been correlated to units in U1395B. Unit ages of 1.75 ka, 6 ka, 14 ka, 66.5 ka, 107 ka, and 130 ka in Hole U1395B at core depths of 0.49 m, 2.52 m, 3.98 m, 6.26 m, 10.47 m, and 18.49 m respectively were used in age model 1. Using oxygen isotope analysis 3 MIS boundaries were identified and used. These are MIS boundaries 6/7 (191 ka), 7/8 (243 ka) and 8/9 (300 ka) at core depths of 28.31 m, 35.93 m, and 43.84 m respectively [Lisiecki and Raymo. 2005]. Finally, two paleomagnetic reversal dates of 781 ka, and 988 ka, at depths of 63.06 m, and 89.08 m are used in age model 1.

Using Age Model 1, the calculated sedimentation rates in the upper 300 ka of Hole U1395B fluctuate between 2 to 17 cm/ka, and encompass the range of hemipelagic sedimentation rates (5 to 10 cm/ka) previously determined in the area [Reid et al., 1996; Watt et al., 2012b]. The greater variability in apparent accumulation rates determined from Age Model 1 (particularly for the lower sedimentation rates) likely reflects the effects of turbidite erosion. Sedimentation rates in age model 1 between 300-988 ka are relatively constant at 3.2-9 cm/ka. The reduction in variability of sedimentation rates further down the core likely reflects the fact that there are fewer dated horizons deeper in Hole U1395B, resulting in a smoother apparent sedimentation rate.

Age Models 2 and 3: Age Model 2 uses Deposit 2 as a boundary at 130 ka (Figure 2; Cassidy et al., [2015]) at 18.49 m, and the paleomagnetic dates of 781 ka, and 988 ka, at depths of 63.06 m, and 89.08 cm respectively. Age Model 3 uses only the two paleomagnetic dates. Using Age Models 2 and 3, estimated sedimentation rates are less variable throughout the core with long-term rates of 4-8 cm/ka.

4.2. Event frequency offshore Montserrat

Events are not distributed regularly through time in core U1395B, but appear to cluster within specific time periods (Figure 4). To better understand this long-term variation in event timing we conduct a moving sum, where the number of events are summed every 50 kyr, at 10 kyr increments. Observations do not change when using bins of 30 kyr and 100 kyr (see Figures S4 and S5). Conservatively, we classify periods of increased frequency as periods where all three age models show that the frequency of event deposits is above the mean 90% confidence interval of the moving sum data (Figure 5). Periods of reduced activity are defined as periods where all three age models show that event frequency is below 1 standard deviation from the mean. In all age models, these periods of relative quiescence last on the order of 10^4- 10^5 kyr. In Hole U1395B, all age models show an increased frequency of all event deposits (above the 90% confidence interval of 8.44 events in 50 ka) between ~170 ka to ~120 ka. This peak in Montserrat's volcanism lies within the period of Soufrière Hills activity (constrained from subaerial dates as 290 ka to present, but see discussion in Section 5.1), and suggests that the largest flank collapse of Soufrière Hills (Deposit 2, at 130 ka) and the South Soufrière Hills basaltic episode (~130 ka) both occurred towards the end of the most active phase of Soufrière Hills' eruptive history.

When examining volcaniclastic deposits only (volcanic turbidites and tephra fall), there are three periods where frequency is greater than the mean 90% confidence interval, between ~930 ka to ~900 ka, ~810 ka to ~760 ka, and ~190 ka to ~120 ka. We interpret periods with a higher frequency of both tephra fall and volcaniclastic turbidites as representing episodes of elevated eruptive activity at Montserrat (Figure 5). The older two periods coincide with activity at Centre Hills volcano, and the younger period (which is similar to that derived from the whole dataset) to Soufrière Hills.

The periods of heightened volcanic activity show a general correlation with changes in the style of eruptions at Montserrat (Figures 4 and 5). The ~810 to ~760 ka increase in event frequency coincides with the appearance of scoria within Hole U1395B. The ~190 ka to ~120 ka increase in event frequency coincides broadly with the onset of activity at South Soufrière Hills [Harford et al., 2002].

To test if there is any correlation between sea-level and turbidite frequency we use a linear model (LM), generalised linear model (GLM), and proportional hazards model (PHM) after binning the data into 10 kyr intervals. For further details on the statistical methods see Hunt et al. [2014] and Clare et al. [2016]. Unit ages are given in Table S4 and test results are given in Table 2.

Statistical analyses are conducted on all three age models in order to test the sensitivity of results to dating errors and to determine if the results are artefacts of the specific age model used. By comparing results from the three age models, the effects of age uncertainty can be better understood. We pose the null hypothesis that turbidite frequency is not correlated with sea-level, and P-values < 0.05 allow us to reject this hypothesis. Table 2 shows that using age model 1 does not show significance in any statistical tests, but using age models 2 and 3 shows significance in all three statistical tests. It should be noted, however, that the correlation coefficient for LM is very low (0.002, 0.085, and 0.077 for age models 1-3 respectively). Low correlation coefficients for age models 2 and 3 indicate that while there may be a broad correlation between sea-level and turbidite frequency, the variation means that the scatter about that trend is very wide. Grouping together of turbidites from eruptive and collapse activity, effects of data binning, or genuine natural noise, may cause this broad scatter. We therefore conclude that all three age models are in agreement and show that there is little to no correlation between sea-level and turbidite frequency. Dating errors are unlikely to affect this observation due to the consistency of this result across all three age models.

Although there appears to be no correlation between turbidite frequency and sea-level, all three of the dated larger landslide deposits from Soufrière Hills volcano (Deposits 1 and 5, 8-14 ka and Deposit 2, 130 ka occur during periods of rapid sea-level rise (>5 m/ka) (Figure 5). Note that older landslides of Centre Hills age are not well dated. Larger landslide deposits, associated with volcanic flank collapse, are easily distinguishable from other eruption-related deposits, unlike turbidites, and there is a better degree of confidence in the dating of these events. We investigate this apparent correlation in a later section using a wider global dataset (*section 5.5.*).

5. Discussion

5.1. How does the submarine record relate to subaerial activity?

Montserrat is part of an active island arc with numerous active volcanoes on other islands, which may be the source of some deposits in the U1395B stratigraphy. For example, site U1395B is situated ~25 km southeast of Montserrat and ~35 km downwind (northwest) of Guadeloupe [Radiosonde wind data], which is thus also a plausible potential source for deposits in the core. Eruptive products from Guadeloupe can be distinguished using lead isotopes because Guadeloupe has a higher radiogenic lead component [Cassidy et al., 2012a; Palmer et al., 2016], and Coussens et al. [2016] use Pb isotopes to show that most tephra layers recorded within Hole U1395 B are likely to be from Montserrat. Over the past 1 Ma [Samper et al., 2007], volcanic activity occurred in the southeast of Guadeloupe at Grande Découverte Soufrière, producing landslides that have mostly travelled westwards into a canyon system [Samper et al., 2007]. The canyon system has accumulated deposits towards the west or southwest of Guadeloupe: thus, landslides and turbidites from Guadeloupe are unlikely to produce deposits within Hole U1395B, and we assume that the majority of visible turbidite layers are from Montserrat.

Limited Ar-Ar dating from on-land samples on Montserrat suggests that volcanism occurred at Centre Hills between ~990–550 ka [Harford et al., 2002] followed by a long hiatus in activity until ~290 ka, when activity commenced at Soufrière Hills. At ~130 ka there was a brief period (~10 kyr) of eruptive activity at the new volcanic centre, South Soufrière Hills, after which activity migrated back to the Soufrière Hills. The apparent gap in subaerial volcanism from ~500-290 ka is not replicated in any of the age models for Hole U1395B (Figures 4 and 5), where the periods of relative quiescence are much shorter, lasting 10^4-10^5 kyr. This suggests that activity migrated relatively rapidly between Centre Hills and Soufrière Hills, and may even have overlapped. This difference between the subaerial and marine records is likely an artefact of limited dating, exposure and erosion of the subaerial record. As such, the offshore stratigraphy provides a higher resolution record and a better means of investigating temporal patterns in volcanic activity in greater detail.

Trofimovs et al. [2006] showed that 90% of the eruptive products from the 1995-2010 eruption of Montserrat had been deposited offshore, supporting our inference that the submarine record is likely to provide a more complete archive of events than the subaerial record. However, deposition in marine settings involves complex transitions between subaerial and submarine transport processes. Thus, although the offshore stratigraphy records more volcanic events than the subaerial record, offshore facies may not provide a truly representative record of a particular type of eruption.

5.2. How does the frequency of collapses relate to volcanism?

Increases in the frequency of tephra fall deposits above the mean 90% confidence interval (3.64 events in 50 ka) indicate that there was more explosive volcanic activity between

~800 ka to ~760 ka (Centre Hills period), and ~230 ka to ~140 ka (Soufrière Hills period) (Figure 5). Turbidite frequency also increases during these periods, but not all observed increases are above the mean 90% confidence interval (Figure 5). These observations are consistent for all age models used, suggesting that these periods of increased volcanism and turbidite frequency are unlikely to be age model artefacts. During periods of effusive volcanic activity (i.e. the lava-dome forming eruptions that typify much of Montserrat's volcanism), there is a greater rate of edifice growth and an increase in the number of volcano-tectonic earthquakes and explosive eruptions, all of which are likely to enhance the likelihood of mass wasting. The largest flank collapse from Soufriere Hills (130 ka) occurred near the end of the peak activity at the centre (whether derived from all core deposits, or tephra fall deposits alone), suggesting that elevated output at this time led to major flank instability.

Bioclastic turbidites show another increase in frequency at ~560 ka to ~500 ka suggesting that other factors may be important in triggering or priming carbonate shelf collapse (Figure 5), such as sea-level change or large earthquakes.

5.3. How does the frequency of collapses at Montserrat relate to sea-level?

Turbidite frequency does not show a statistically robust correlation with eustatic sea-level changes (in all age models), but all three of the well-dated large-scale landslides (>0.3 km^3) from Montserrat (Deposits 1, 2 and 5) occurred during periods of rapid (>5 m/ka) global sea-level rise (Figure 5) [Miller et al., 2005]. Deposits 1 and 5 (dated between 14-8 ka) coincide with rapid sea-level rise at 15 ka to 5 ka, from 60 m to 1.6 m below present day sea-level (Figure 5). Deposit 2 is dated at 130 ka, which coincides with a second period of rapid sea-level rise at 130 ka to 120 ka (Figure 5). Although this is a small number of events, the record suggests that rapid sea-level rise may trigger or precondition the flank collapses on Montserrat.

5.4. Large-scale flank collapse: constructing a global landslide record.

To investigate if large landslide occurrences during rapid sea-level rise are replicated more widely, we have compiled a global dataset of landslide ages at volcanic islands over the past 1 Ma, building on the compilation by Quidelleur et al., [2008]. The compiled global data set has 25 ages from volcanic islands (errors <±22.5 ka) that are constrained within errors of ±22.5 ka, comprising 9 from ocean islands and 16 from island arcs (Tables 3 and 4).

Many landslides have large age uncertainties, and if age errors are too large (i.e., on the order of sea-level cycles) then relationships between sea level, volcanism, and landslides cannot be determined [Pope et al., 2015]. Our age-uncertainty criterion of <± 22.5 ka has been selected on this basis, because it provides a sufficiently large dataset to observe potential patterns, with age errors that are a similar order of magnitude to the periodicity of sea-level cycles (10^3-10^4 yrs).

5.4.1 Ocean islands

Multiple large-scale landslide deposits dating back to at least 22 Ma lie offshore the Canary Islands [Stillman, 1999]. The oldest well-dated landslide from the island of El Hierro is El Julan, to the SW (130 km^3) [Gee et al., 2001]. Onshore there is an 8 km wide scar, with infilling material dated at <158 ± 4 ka [Guillou et al., 1996]. Turbidite P, in the Madeira Abyssal Plain, is dated at 540 ± 10 ka using biostratigraphy, and is correlated to the El Julan landslide based on geochemistry and subaerial date constraints [Hunt et al., 2013], and is our best age estimate of the El Julan collapse. North of El Hierro lies the El Golfo deposit (150 km^3) [Urgeles et al., 1997], which is correlated with a large (14.5 km wide) subaerial crater [Urgeles et al., 1997]. This scar is dated between 87± 8 ka and 11 ± 7 ka using Ar-Ar dating of material that are incised by and infill the scar [Guillou et al., 1996]. In the Madeira Abyssal Plain turbidite B is correlated with the El Golfo collapse [Hunt et al., 2013] and is dated at 15 ± 5 ka [Weaver et al., 1992; Hunt et al., 2013] using biostratigraphy of surrounding hemipelagic material. We use the age of turbidite B for the date of the El Golfo collapse in this study.

The Icod, Orotava and Guimar landslides are the best-dated landslides from Tenerife. The Guimar landslide (120 km^3) [Krastel et al., 2001] correlates with turbidite Z in the Madeira Abyssal Basin [Hunt et al., 2013], which places the events via biostratigraphic ages at 850±10 ka. The Orotava and Icod landslides, north of Tenerife, correlate with large amphitheatre-shaped depressions. The minimum age of the Orotava landslide is deduced from the oldest lava flow (PS4) infilling the Orotava Valley (534±9 ka) [Boulesteix et al., 2013], and the maximum age from lavas intersected by the landslide scar (558±8 ka). The landslide also correlates with turbidite MO in the Madeira Abyssal Plain, dated at 540±5 ka using biostratigraphy [Hunt et al., 2013]. Subaerial dating suggests the Icod landslide occurred between 175±3 ka and 161±5 ka by K-Ar dating material that are incised by and infill the landslide scar respectively [Boulesteix et al., 2011] but more recently Hunt et al., [2013] used turbidite G in the Madeira Abyssal Plain to obtain a biostratigraphic age of 165±5 ka, which we use here.

Offshore La Palma, the Cumbre Nueva landslide is well-dated. The headwall of the landslide has been identified as the prominent Cumbre Nueva Ridge that encloses a horseshoe-shaped depression [Urgeles et al., 1999]. The Cumbre Nueva landslide is thought to have occurred after the emplacement of the Upper Taburiente volcanic deposits (566±8 ka) and was followed by the emplacement of the Bejenado volcano (537±8 ka) in the landslide scar [Guillou et al., 1998, 2001; Carraceado et al., 2001]. Hunt et al [2013] date the Cumbre Nueva landslide at 480±5 ka by correlating the landslide with turbidite N in the Madeira Abyssal Plain. This contrasts with subaerial dating, and we preferentially use the subaerial dates, because turbidite N may correlate with a younger landslide from La Palma.

To the east of Pico del Fogo in the Cape Verde Islands is a 130-160 km^3 landslide deposit [Lebas et al., 2007; Masson et al., 2008], which has been correlated with fields of boulders and chaotic conglomerates (interpreted as tsunami deposits) on the nearby island of Santiago [Ramalho et al., 2015]. ^{3}He dating of these tsunami deposits suggests a landslide age of 73±7 ka [Ramalho et al., 2015]. This is close in age to a post collapse lava flow on Pico del Fogo dated at 86±3 ka [Paris et al., 2011].

In the Hawaiian Archipelago at least 68 large volume landslides (up to 5000 km^3) have been identified [Moore et al., 1989, 1994]. However, only the Alika 2 deposit, offshore Mauna Loa, is well dated. Cores F88 B-13, F91 39B1 and F91 4082 sample the Alika 2 deposit. Planktonic forams within the Alika 2 deposit date the landslide at 127±5 ka using oxygen isotope stratigraphy [McMurty et al., 1999].

The island of Tahiti has two horseshoe shaped depressions to the north and south of the island that correlate with large hummocky landslide deposits offshore with respective volumes of 800 km^3 and 1150 km^3 [Hildenbrand et al., 2004]. The Tahitian shield was constructed between 1.4-8.7 Ma [Hildenbrand et al., 2004], with vent locations concentrated along an E-W rift down the centre of the island. Late activity along these vents (~870 ka) is thought to have triggered the two landslides [Hildenbrand et al., 2004]. After the landslides, activity moved to the north, infilling the northern crater (851±11 ka) [Hildenbrand et al., 2004]. We therefore assume an age range for the northern landslide between 870 to 851±11 ka. The southern crater is dated at ~500 ka, but is too poorly constrained to be included in the database.

5.4.2 Island Arc Landslides

Evidence of large landslides has been identified at several islands in the Lesser Antilles (in addition to Montserrat). At Guadeloupe, subaerial exposures allow two events, the Carmichael and Carbet landslides, to be well dated [Boudon et al., 1984, 1987, 2007]. The Carmichael landslide covers 17 km^2 onshore, and large blocky deposits are observed offshore [Boudon et al., 1984]. The landslide is thought to be associated with the Carmichael crater that has a volume of 0.3 km^3. Uncarbonised wood found within the deposit yields ^{14}C ages of 8400 ±1500 to 11270±185 BP [Boudon et al., 1984]. The Carbet landslide (estimated volume of 0.5 km^3) is dated by subaerial outcrops along the Rivière du Carbet, where uncarbonised wood within the deposits yielded ^{14}C dates between 2800-3450 BP [Boudon et al., 1984, 2007; Daigun et al., 1981].

On Dominica four large landslides are observed, but only the Soufriere event is well dated. The Soufriere event (estimated volume 6-7 km^3) formed from the collapse of the Plat Pays volcanic edifice [Le Friant et al., 2002]. The lower bound age constraint is from ^{14}C dating of carbonaceous material found within a pyroclastic flow deposit from the Plat-Pays volcano dated at 6600±50 ka. An upper bound comes from ^{14}C dating material

(2380± 75 ka) from a tephra fall that overlies a mega block from the landslide (Scotts Head) [Le Friant et al., 2002].

On Martinique, three of the four large landslide deposits are well dated (D1, D2 and D3). The D1 event is associated with a large west-facing landslide scar and has an estimated volume of 25 km^3. The northern rim of the crater is well exposed, but the southern rim may have been destroyed and/or covered by later landslide events [Boudon et al., 2007]. K-Ar dating of material infilling and incised by the landslide scar are dated at 126±2 ka and 127±2 ka respectively. The D2, or St Pierre event formed a large west-facing amphitheatre-shaped structure and produced an offshore deposit with a volume of >13 km^3. The upper bound date is given by U-Th disequilibrium dating of material intersected/outside the D2 structure, yielding ages of 37±4 ka (Mont Calebasse lava dome) and 25±1 ka (Mourne Plumé lava dome) [Le Friant et al., 2003]. The lower bound age, of 25 000±1040 years, is given by a ^{14}C charcoal age from a scoria flow deposit that in-fills the D2 structure [Vincent et al 1989]. D3, or the Rivière Sèche event, has an estimated volume of 2 km^3. The Aileron lava dome (summit part of Montagne Pelée) is intersected by the D3 structure and is dated at 9.7±0.5 ka, providing an upper age limit [Le Friant et al., 2003]. The "Sans Nom" lava dome in-fills the D3 structure and is dated at 9±1 ka [Le Friant et al., 2003].

Further afield, multiple large landslide deposits have been identified on and offshore Ischia, Italy [Chiocci and de Alteriis 2006; De Alteriis and Violante, 2009], five of which are well dated. The South landslide (1.5 km^3) is correlated with the offshore DF1 deposit and is dated at 2.4-3 ka (^{14}C on planktonic forams within hemipelagic material above and below DF1) [De Alteriis et al., 2010]. The Falanga and Pietre Rosse landslides outcrop to the east of Ischia, with a combined offshore volume of 11 km^3. The Falanga deposit is dated at 400 BC based on historical chronicles [Buchner 1986]. The Pietre Rosse landslide has a maximum age constraint as it overlies the Citara Formation 40 ka [Vezzoli 1988], and the upper bound age is given by the overlying Falanga landslide.

To the north of Ischia two large landslide deposits (NDDe and NDDw) are seen [De Alteriis and Violante 2009]. The NDDe correlates onshore with the Casamicciola and Lacco Ameno landslide deposits [Seta et al., 2012]. The Lacco Ameno deposit is poorly dated and is not included within the global database. The Casamicciola deposit overlies the Punta La Scrofa Tuff, dated at <800 BC [De Vita et al., 2010]. Within seismic reflection profiles, a horizon beneath NDDw has been correlated with the onshore Zaro lava flow, dated at 6±2 ka and 9±1 ka using K-Ar dating [Vezzoli et al., de Aleriis and Violante, 2009]. Although the Casamicciola and NDDw have no upper bounds, the ages are within the error of ± 22.5 kyr, and so are included within the global dataset.

The Japanese volcano of Usu is situated in the South of the Japanese island of Hokkaido. Usu formed ~20 ka [Soya et al., 2007] and after the edifice reached 1000 m there was a large summit collapse (1-2 km^3). This collapse, named the Zenkojii collapse, occurred at ~7-8 ka based on subaerial dating of infilling and cross-cut deposits [Moriya, 2003 (in Japanese); Soya et al., 2007].

A large 5 km^3 collapse from Ritter island (offshore New Guinea), which occurred 13th March 1888, is also included in the global database [Cooke 1981; Ward and Day 2003].

5.5. Large-scale flank collapse and sea-level: comparison to global records

At Montserrat, the three well-dated large landslides from Soufrière Hills coincide with periods of rapid sea level rise. Using the global compilation, box and whisker plots (Figure 6) show that landslide occurrences at other island volcanoes are skewed towards periods of more rapid sea-level rise. In contrast, at ocean islands the distribution of event timing shows no clear correlation with specific regimes of sea level (Figure 6). This is supported by preliminary statistical analyses (Mann-Whitney and Kolmogorov-Smirnov tests, see supplementary information).

The global data set of landslide ages is restricted (9 events from ocean islands, 16 events from island arcs). Dating landslide deposits is challenging, because most material is emplaced offshore in poorly accessible, deep marine settings, typically comprising chaotic mixtures of material. Direct dating of material within landslides only provides maximum age constraints of landslide emplacement, unless material such as vegetation incorporated into the landslide deposits can be identified and dated. Indirect dating of material overlying and underlying landslide deposits or scars can result in large age gaps. Consequently the global landslide database is sparse, and dominated by a very few well-studied regions (e.g. Ischia, Lesser Antilles). Even in other regions where numerous events have been identified (e.g. Aleutian Islands; Coombs et al. [2007]), very few events are dated, and so are excluded from our dataset.

Given the limitations of a restricted dataset, it is thus difficult to test the strength of the observed correlation between event timing and sea level change. Furthermore the island arc database is biased towards recent landslide events (<20 ka), which includes a period of rapid sea-level rise (Figure 6). Thus the apparent prevalence of island arc landslides during periods of rapid sea-level rise could also be affected by a temporal record bias. Further investigation (by substantially increasing the dated landslide database) is required to test this initial result, which suggests a difference between how sea level change influences flank stability in island arc and ocean island settings.

Nevertheless, it is worth briefly considering the processes by which sea level rise may increase the likelihood of flank collapse at island-arc volcanoes. A ~100 m rise in sea level potentially enhances both dyke ascent (and hence volcanism) and fault movement in island-arc settings [cf. Nakada and Yokose, 1992], although the relationship between volcanism and sea level change may be complex [McGuire et al., 1997] and is incompletely understood. Overpressure in magma chambers, which decreases by viscoelastic relaxation, is more sensitive to loading rate than the absolute load [Jellinek et al., 2004] consistent with the observed correlation of collapse rapid sea-level rise. Furthermore, sealevel rise may result in greater magma- water interaction encouraging explosive, phreatomagmatic behaviour. Such explosive behaviour may reduce flank stabitlity. An incipient instability within a volcanic edifice may also move closer to a critical failure point due either to direct stress increases associated with sea-level rise, possibly combined with other factors. These may include enhanced erosion and modification of the groundwater system associated with rapid sea-level change. Although the consequence of sea-level rise on groundwater may depend on local factors, pore-pressure increases within hydrothermal systems have been suggested as a cause of edifice collapse [Elsworth and Voight, 1995; Day, 1996; Reid, 2004].

Our results suggest that these factors may be less significant in ocean-island settings, but the reason for this is as yet unclear. Structurally, the more basaltic composition of ocean islands means they are likely to have more stable flanks than island arcs, with a broader profile and lower slope gradients [Watt et al., 2014], yet the presence of widespread landslide deposits around many ocean islands indicates that they are still prone to catastrophic flank failure.

6. Conclusions

In contrast to the subaerial stratigraphic record, volcaniclastic layers within IODP Hole U1395B provide a more complete record of volcanism on Montserrat. Periods of reduced event frequency (interpreted as periods of volcanic quiescence) last of the order $10^4 - 10^5$ ka, substantially less than apparent gaps in the subaerial record. The pauses in activity suggested by the subaerial record are likely to be a manifestation of poor preservation and burial of onshore stratigraphy, coupled with the predominantly offshore deposition of volcanic products. The marine record reveals that three periods of heightened volcanic activity at Montserrat occurred at ~930 ka to ~900 ka, ~810ka to ~760 ka (both during the Centre Hills period), and ~190 ka to ~120 ka (during the Soufrière Hills period). A notable increase in event frequency at ~810 ka to ~760 ka coincides with the occurrence of mafic scoria in Hole U1395B, while the peak in Soufrière Hills volcanism coincides with the largest flank collapse from the volcano (130 ka) and a brief switch to mafic volcanism.

Periods of heightened volcanic activity coincide with periods of increased turbidite occurrence, suggesting that intensified volcanic activity may facilitate mass-wasting processes. No statistically significant correlation of turbidite occurrence (collapse frequency) and sea level were observed, but all of the well-dated and large-scale landslides on Montserrat occurred during periods of rapid sea-level rise. While the global dataset is small and there are uncertainties associated with dating landslide events, this pattern of large-scale landslides coinciding with periods of rapid sea-level rise is replicated within a global data set for island-arc volcanoes, but not at ocean islands. The reasons for this difference between island arcs and ocean islands remain unclear, but may reflect a greater susceptibility of the steeper, more lithologically diverse flanks of island-arc volcanoes to rapid sea-level changes, relative to ocean islands.

7. Acknowledgements

We would like to thank all of the members on the Expedition 340 science party for their hard work during and after the cruise. We would also like to thank the captain of the RN *JOIDES Resolution* and the crew, staff, and the shipboard scientists of Expedition 340 for their work during the cruise. Many thanks to the staff at Texas Agricultural and Mechanical University who sampled Hole U1395B. Mike Cassidy acknowledges a Alexander Von Humboldt grant. SW acknowledges NERC grants NE/K000403/1 and NE/I02044X/1. Radiocarbon dates were funded by NERC under allocation SUERC 1721.0513 at the NERC radiocarbon facility. Thanks to Suzanne MacLachlan in BOSCORF for providing lab space and equipment. Finally thanks to the two anonymous reviewers for their insightful feedback. Supporting data has been included in four supplementary tables, a supplementary information file, and a supplementary figure file. Any further data can be obtained from Maya Coussens (mfc1e12@soton.ac.uk or maya.pratt@mail.com) and IODP LIMS reports (http://web.iodp.tamu.edu/UWQ/).

8. References

Ablay, G. J. and J. Marti (2000), Stratigraphy, structure, and volcanic evolution of the Pico Teide-Pico Viejo formation, Tenerife, Canary Islands, *Journal of Volcanology and Geothermal Research, 103*, 175-208

Ancochea, E., J. M. Fuster, E. Ibarrola, A. Cendrero, J. Coello, F. Hernan, J. M. Cantagrel, C. Jamond (1990), Evolution of the island of Tenerife (Canary Islands) in the light of new K-Ar data, *Journal of Volcanology and Geothermal Research*, 44, 231-249, doi: 0377-0273/90/$03.50

Boudon, G., M. P. Semet, and P. M. Vincent (1984), Flank failure–directed blast eruption at Soufrière, Guadeloupe, French West Indies: A 3,000-yr-old Mt. St. Helens?, *Geology*, *12*(6), 350-353

Boudon, G., M. P. Semet, and P. M. Vincent (1987), Magma and hydrothermally driven sector collapses: The 3100 and 11,500 y. BP eruptions of la Grande Decouverte (la Soufrière) volcano, Guadeloupe, French West Indies, *Journal of volcanology and geothermal research*, *33*(4), 317-323

Boudon, G., A. Le Friant, J. C. Komorowski, C. Deplus and M. P. Semet (2007), Volcano flank instability in the Lesser Antilles Arc: Diversity of scale, processes, and temporal recurrence, *Journal of Geophysical Research, 112*, B08205, doi:10.1029/2006JB004674

Boulesteix. T., A. Hildenbrand, P-Y. Gillot and V. Soler (2011), Eruptive response of oceanic islands to giant landslides: New insights from the geomorphologic evolution of the Teide–Pico Viejo volcanic complex (Tenerife, Canary), *Geomorphology, 138,61-73*

Buchner, G. (1986), Eruzioni vulcaniche e fenomeni vulcano-tettonici di età preistorica e storica nell' isola di Ischia, *In Tremblements de terre, éruptions volcaniques et vie des hommes dans la Campanie antique, vol, 7,* edited by C. Albore-Livadie, *Publishe by Centre Jean Bérard*, Napoli, 145–188

Cande, S.C., D. V. Kent, 1992a. A new geomagnetic polarity time scale for the Late Cretaceous and Cenozoic, *Journal of Geophysical Research* 97, 13917-13951

Cande, S.C., D. V. Kent, 1992b, Ultrahigh resolution of marine magnetic anomaly profiles: A record of continuous paleointensity variations?, *Journal of Geophysical Research* 97, 15075-15083

Cande. S. C., D. V. Kent (1995), Revised calibration of the geomagnetic polarity timescale for the Late Cretaceous and Cenozoic, *Journal of Geophysical Research, 100(B4),* 6093-6095

Carracedo, J. C. (1999), Growth, structure, instability and collapse of Canarian volcanoes and comparisons with Hawaiian volcanoes, *Journal of Volcanology and Geothermal Research,* 94(1), 1–19.

Cassidy, M., R. N. Taylor., M. R. Palmer., R. Cooper., C. Stenlake., J. Trofimovs (2012a) Tracking the magmatic evolution of an island arc volcano: Insights from a high-precision Pb isotope record of Montserrat, Lesser Antilles, *Geochemistry, Geophysics, Geosystems,* 13, Q05003 doi:10.1029/2012GC004064

Cassidy, M., J. Trofimovs, S. F. L. Watt, M. R. Palmer, R. N. Taylor, T. M. Gernon, P.J. Talling and A. Le Friant (2012b), Multi-stage collapse events in the South Soufrière Hills, Montserrat, as recorded in marine sediment cores, *In the eruption of Soufrière Hills Volcano, Montserrat from 2000-2010,* Edited by G. Wadge, G., et al., *The Geological Society Special Publications*, *39*, 383-397

Cassidy, M., J. Trofimovs, M. R. Palmer, P. J. Talling, S. F. L. Watt, S. G. Moreton and R. N. Taylor (2013), Timing and emplacement dynamics of newly recognised mass flow deposits at ~8-12 ka offshore Soufrière Hills volcano, Montserrat: How submarine stratigraphy can complement subaerial eruption histories, *Journal of Volcanology and Geothermal Research, 253,* 1–14, doi:10.1016/j.jvolgeores.2012.12.002

Cassidy, M., S. F. L. Watt, M. R. Palmer, J. Trofimovs, W. Symons, S. E. Maclachlan and A. J. Stinton (2014), Construction of volcanic records from marine sediment cores: A review and case study (Montserrat, West Indies), *Earth-Science Reviews, 138*, 137–155, doi:10.1016/j.earscirev.2014.08.008

Cassidy. M., et al., (2015), Rapid onset of mafic magmatism facilitated by volcanic edifice collapse, *Geophysical Research Letters, 42(12),* 4778-4785

Clare, M. A, P. J. Talling, P. H. Challenor and J. E. Hunt, (2016). Tempo and triggering of large submarine landslides - Statsitical analysis for hazard assessment. In Submarine Mass Movements and Their Consequences, edited by G. Lamarche et al., . Springer, 41, 509-517

Cole, P. D., E. S. Calder, R. S. J. Sparks, A. B. Clarke, T. H. Druitt, S. R. Young and G. E. Norton (2002), Deposits from dome-collapse and fountain-collapse pyroclastic flows at Soufrière Hills Volcano, Montserrat, G*eological Society, London, Memoirs,* 21(1), 231-262

Collins, B. D. and T. Dunne (1986), Erosion of tephra from the 1980 eruption of Mount St. Helens, *Geological Society of America Bulletin*, *97*(7), 896-905

Cooke, R.J.S. (1981), Eruptive history of the volcano at Ritter Is- land, in Cooke–Ravian Volume of Volcanological Papers, *In Geological Survey of Papua New Guinea Memoir*, edited by R. W. Johnson, 10, 115-123

Coombs, M. L., S. M. White and D. W. Scholl, (2007), Massive edifice failure at Aleutian arc volcanoes, *Earth and Planetary Science Letters,* 256(3), 403-418

Coussens M, et al., (2016), Synthesis: stratigraphy and age control for IODP Sites U1394, U1395, and U1396 offshore Montserrat in the Lesser Antilles. *In Proceedings of the Integrated Ocean Drilling Program,* principal investiagators A. Le Friant, O. Ishizuka, N. A. Stroncik, Volume 340

Crutchley, G. J., J. Karstens, C. Berndt, P. J. Talling, S. F. L. Watt, M. E. Vardy, V. Huhnerbach, M. Urlaub, S. Sarkar, D. Klaeschen, M. Paulatto, A. Le Friant, E. Lebas and F. Maeno (2013), Insights into the emplacement dynamics of volcanic landslides from high-resolution 3D seismic data acquired offshore Montserrat, Lesser Antillies, *Marine Geology, 335*,1-15, doi:10.1016/j.margeo.2012.10.004

Dagain, J. (1981), La mise en place du massif volcanique Madaleine—Soufrière, Basse-Terre de Guadeloupe, Antilles [3rd cycle thesis]: Orsay, France, Université Paris Sud

Dagain, J., M. Paterne, and D. Westercamp (1981), La mise en place du massif Madeleine-Soufrière, Basse-Terre de Guadeloupe, A*ntilles: Académie des Sciences, Comptes Rendus*, 11 (292), 921-926

Day, S. J. (1996), Hydrothermal pore fluid pressure and the stability of porous, permeable volcanoes. *In Volcano Instability on the Earth and Other Planets*, edited by W. J. McGuire, A. P. Jones, *Geological Society Special Publication*, 110, 77-93

De Alteriis, G. and C. Violante (2009), Catastrophic landslides off Ischia volcanic island (Italy) during prehistory, *Geological Society, London, Special Publications*, 322(1), 73-104

De Alteris, G., D. D. Insinga, S. Morabito, V. Morra, F. L. Chiocci, F. Terrasi, C. Lubritto, C. Di Benedetto and M. Pazzaneses (2010), Age of submarine debris avalanches and tephrostratigraphy offshore Ischia Island, Tyrrhenian Sea, Italy, *Marine Geology,* 278, 1-18, doi:10.1016/j.margeo.2010.08.004

Deplus, C., A. Le Friant, G. Boudon, J. C. Komorowski, B. Villement, C. Harford, J. Segoufin and J. L. Chiminee (2001), Submarine evidence for large-scale debris avalanches in the Lesser Antillies Arc, *Earth and Planetary Science Letters, 192,* 145-157

De Vita, S., F. Sansivero, G. Orsi, E. Marotta and M. Piochi (2010), Volcanological and structural evolution of the Ischia resurgent caldera (Italy) over the past 10 ky. *Geological Society of America Special Papers*, 464, 193-239

Elsworth. D and B. Voight, (1995), Dike intrusion as a trigger for large earthquakes and the failure of volcano flanks, *Journal of Geophysical Research*, 100, 6005-6024

Folk, R. L. and W. C. Ward (1957), Brazos River bar: a study in the significance of grain size parameters, *Journal of Sedimentary Petrology, 27,* 3-26

Gee, M. J. R., D. G. Masson, A. B. Watts and P. A. Allen (2001), The Saharan Debris Flow: an insight into the mechanics of long runout debris flows, *Sedimentology*, 46, 317-335

Gee, M. J. R., A. B. Watts, D. G. Masson and N. C. Mitchell (2001), Landslides and the evolution of El Hierro in the Canary Islands, *Marine Geology*, 177, 271-293

Germa, A., X. Quidelleur, S. Labanieh, P. Lahitte and C. Chauvel (2010), The eruptive history of Morne Jacob volcano (Martinique Island, French West Indies): Geochronology, geomorphology and geochemistry of the earliest volcanism in the recent Lesser Antilles arc, *Journal of Volcanology and Geothermal Research, 198(3-4),* 297–310, doi:10.1016/j.jvolgeores.2010.09.013

Germa. A., X. Quidelleur, P. Lahitte, S. Labanieh, C. Chauvel (2011), The K-Ar Cassignol-Gillot technique applied to wester Martinique lavas: A record of Lesser Antilles arc activity from 2 Ma to Mount Pelee volcanism, *Quaternary Geology*, 6, 341-355

Green, S.B. (1991), How many subjects does it take to do a regression analysis? *In Multivariate Behavioral Research*, 26, 499-510.

Guillou, H., J. C. Carracedo, F. P. Torrado, and E. R. Badiola (1996), K-Ar ages and magnetic stratigraphy of a hotspot-induced, fast grown oceanic island: El Hierro, Canary Islands, *Journal of Volcanology and Geothermal Research*, 73(1), 141-155

Guillou, H., J. C. Carracedo and S. J. Day (1998), Dating of the upper Pleistocene–Holocene volcanic activity of La Palma using the unspiked K–Ar technique, *Journal of Volcanology and Geothermal Research*, 86(1), 137-149

Guillou, H., J. C. Carracedo and R. A. Duncan(2001), K–Ar, 40 Ar–39 Ar ages and magnetostratigraphy of Brunhes and Matuyama lava sequences from La Palma Island, *Journal of Volcanology and Geothermal Research*, 106(3), 175-194

Hatfield. R. and Expedition 340 Scientists (2013), Paleomagnetism in methods, *In Proceedings of IODP, 340: Tokyo (Integrated Ocean Drilling Program Management International, Inc.),* Edited by A. Le Friant, O. Ishizuka, N. A. Stroncik, and the Expedition 340 Scientists, doi:10.2204/iodp.proc.340.102.2013

Harford, C. L., M. S. Pringle, R. S. J. Sparks and S. R. Young (2002), The volcanic evolution of Montserrat using 40Ar/39Ar geochronology, *Geological Society, London, Memoirs*, *21*, 93–113, doi: 10.1144/GSL.MEM.2002.021.01.05

Herd, R.A., M. Edmonds and V. Bass (2006). Catastrophic lava dome failure at Soufriere Hills Volcano, Montserrat 12–13 July 2003, *Journal of Volcanology and Geothermal Research*, 148, 234–252

Hildenbrand. A., Gillot. P-Y., Le Roy. I. (2004). Volcano-tectonic and geochemical evolution of an oceanic intra-plate volcano: Tahiti-Nui (French Polynesia), *Earth and Planetary Science Letters*, 217, 349-365

Houghton, B. F., C. J. N. Wilson, M. O. McWilliams, M. A. Lanphere, S. D. Weaver, R. M. Briggs and M. S. Pringle (1995), Volcanic Zone , New Zealand Chronology and dynamics of a large silicic magmatic system : Central Taupo Volcanic Zone , New

Zealand, *Geology, 23*, 13–16, doi: 10.1130/00917613(1995)023<0013:CADOAL>2.3.CO;2

Hunt, J. E., R. B. Wynn, P. J. Talling and D. G. Masson (2013), Turbidite record of frequency and source of large volume (>100 km^3) Canary Island landslides in the last 1.5 Ma: Implications for landslide triggers and geohazards, *Geochemistry, Geophysics, Geosystems*, *14(7)*, 2100–2123, doi: 10.1002/ggge.20139

Hunt, J. E., P. J. Talling, M. Clare, I. Jarvis, and R. B. Wynn (2014), Long-term (17 Ma) turbidite record of the timing and frequency of large flank collapses of the Canary Islands, *Geochemistry, Geophysics, Geosystems, 15,*3322–3345, doi: 10.1002/2014GC005232

Jellinek, A.M., M. Manga, and M.O. Saar (2004) Did melting glaciers cause volcanic eruptions in eastern California? Probing the mechanics of dike formation, *Journal of Geophysical Research*, 109, B09206, doi:10.1029/2004JB002978.

Jutzeler, M., J. D. L. White, P. J. Talling, M. McCanta, S. Morgan, A. Le Friant and O. Ishizuka (2014), Coring disturbances in IODP poston cores with implication for offshore record of volcanic events and the Missoula megafloods *Geochemistry, Geophysics, Geosystems,* 3572-3590, doi: 10.1002/2014GC005447

Kameo, K. and T. J. Bralower (1998), Neogene calcareous nannofossil biostratigraphy of sites 998, 999, and 1000, Caribbean Sea, *Proceedings of the Ocean Drilling Program, Scientifc Results*, *165*,3–17

Keefer, D. K. (2000), Statistical analysis of an earthquake-induced landslide distribution—the 1989 Loma Prieta, California event, *Engineering Geology*, 58(3), 231-249

Kokelaar, B. P. (2002), Setting, chronology and consequences of the eruption of Soufrière Hills Volcano, Montserrat (1995-1999). I*n the eruption of Soufrière Hills volcano, Montserrat, from 1995 to 1991*, edited by T. Druitt, and P. Kokelaar, *Geological Society Special Publications, 21*,1–43, doi: 10.1144/GSL.MEM.2002.021.01.02

Krastel, S., H. U. Schmincke, C. L. Jacobs, R. Rihm, T. P. Le Bas, and B. Alibés (2001), Submarine landslides around the Canary Islands, *Journal of Geophysical Research*, 106 (B3), 3977-3997, doi: 2000JB900413. 0148-0227/01/2000 JB900413$09.00

Lebas, E., S. F. L. Watt, P. J. Talling, N. Feuillet, C. Deplus, C. Berndt and M. Vardy (2011), Multiple widespread landslides during the long-term evolution of a volcanic island: Insights from high-resolution seismic data, Montserrat, Lesser Antilles, *Geochemistry Geophysics Geosystems*, *12(5)*, Q05006, doi:10.1029/2010GC003451

Le Friant, A., Boudon, G., Komorowski, J.-C., Deplus, C. (2002), L'île de la Dominique, à l'origine des avalanches de débris les plus volumineuses de l'arc des Petites Antilles, *C.R. Geosci*, 334, 235–243

Le Friant, A., G. Boudon, C. Deplus and B. Villement (2003), Large-scale flank collapse events during the activity of Montagne Pelée, Martinique, Lesser Antilles, *Journal of Geophysical Research, 108 (B1)*, 2055, doi:10.1029/2001JB001624

Le Friant, A., E. J. Lock, M. B. Hart, G. Boudon, R. S. J. Sparks, M. J. Leng, C. W. Smart, J. C. Komorowski, C. Deplus, J. K. Fisher (2008), Late Pleistocene tephrochronology of marine sediments adjacent to Montserrat, Lesser Antilles volcanic arc, *Journal of the Geological Society*, *165(1)*, 279–289, doi:10.1144/0016-76492007-019

Le Friant, A., C. Deplus and G. Boudon (2009), Submarine deposition of volcanicastic material from the 1995-2005 eruptions of Soufrière Hills volcano, Montserrat, *Journal of the Geological Society, 166*, 171-182, doi: 10.1144/0016-76492008-047

Le Friant, A., C. Deplus, G. Boudon, N. Feuliiet, J. Trofimovs, J. C. Komorowski, R. S. J. Sparks, P. J. Talling, S. Loughlin, M. R. Palmer and G. Ryan (2010), Eruption of Soufrière Hills (1995- 2009) from an offshore perspective: Insights from repeated swath bathymetry surveys, *Geophysical research letters*, *37*, L11307, doi:10.1029/2010GL043580

Le Friant, A., E. Lebas, V. Clement, G. Boudon, C. Deplus, B. de Voogd and P. Bachélery (2011), A new model for the evolution of la Reunion volcanic complex from complete geophysical surveys, *Geophysical Research Letters, 38,* L09312, doi:10.1029/2011GL047489

Le Friant, A., O. Ishizuka, N. A. Stroncik, A. L. Slagle, S. Morgan, T. Adachi, M. Aljahdali and G. Boudon (2012), Lesser Antillies Volcanism and Landslides. Implications for hazard assessment and long-term magmatic evolution of the arc, *Integrated Ocean Drilling Program, Expedition 340 preliminary report,* doi:10.2204/iodp.pr.340.2012

Le Friant, A., et al., (2015), Submarine record of volcanic island construction and collapse in the Lesser Antilles arc: First scientific drilling of submarine volcanic island landslides by IODP Expedition 340, *Geochemistry, Geophysics, Geosystems, 16*, 420–442, doi:10.1002/ 2014GC005652

Lehmann, E. L. and H. J. D'Abrera (2006), Nonparametrics: statistical methods based on ranks, *Springer,* 464, New York

Lénat, J, F., P. Boivin, C. Deniel, P. Y. Gillot, P. Bachèlery, and Fournaise 2 Team (2009), Age and nature of deposits on the submarine flanks of Piton de la Fournaise (Reunion Island), *Journal of Volcanology and Geothermal Research*, 184, 199–207

Lisiecki, L. E. and M. E. Raymo (2005), A Pliocene-Pleistocene stack of 57 globally distributed benthic $\delta^{18}O$ records, *Paleoceanography*, *20*,1–17, doi:10.1029/2004PA001071

Longpré, M. A., J. P. Chadwick, J. Wijbrans and R. Iping (2011), Age of the El Golfo debris avalanche, El Hierro (Canary Islands): New constraints from laser and furnace $^{40}Ar/^{39}Ar$ dating, *Journal of Volcanology and Geothermal Research, 203*, 76-80, doi:10.1016/j.jvolgeores.2011.04.002

Major, J. J., T. C. Pierson., R. L. Dinehart and J. E. Costa (2000), Sediment yield following severe volcanic disturbance—a two-decade perspective from Mount St. Helens, *Geology*, 28(9), 819-822

Marques, R., J. Zêzere., R. Trigo., J. Gaspar and I. Trigo (2008), Rainfall patterns and critical values associated with landslides in Povoação County (São Miguel Island, Azores): relationships with the North Atlantic Oscillation, *Hydrological Processes*, 22(4), 478

Masson, D. G., (1996), Catastrphic collapse of the volcanic island of Hierro 15 ka ago and the history of landslides in the Canary islands, *Geology*, 24 (3), 231-234

Masson, D. G., A. B. Watts, M. J. R. Gee, R. Urgeles, N. C. Mitchell, T. P. Le Bas, and M. Canals (2002), Slope failures on the flanks of the western Canary Islands, *Earth Science Reviews, 57*, 1-35, PII: S0012-8252Ž01.00069-1

Masson, D. G., C. B. Harbitz, R. B. Wynn, G. Pedersen and F. Lovholt (2006), Submarine landslides: processes, triggers and hazard prediction, *Philosophical Transactions of the Royal Society, 364*, 2009-2039, doi:10.1098/rsta.2006.1810

Masson, D. G., T. P. Le Bas, I. Grevemeyer and W. Weinrebe (2008), Flank collapse and large‐scale landsliding in the Cape Verde Islands, off West Africa, *Geochemistry, Geophysics, Geosystems*, 9(7)

McGuire, W. J, R. J. Howarth, C. R. Firth, A. R. Solow, A. D. Pullen, S. J. Saunders, I. S. Stewart, and C. Vita-Finzi (1997), Correlation between rate of sea-level change and frequency of explosive volcanism in the Mediterranean. *Nature,* 389, 473 - 477.

McMurty, G. M., E. Herrero-Bervera, M. D. Cremer, J. R. Smith, J. Resig, C. Sherman and M. E. Torresan (1999), Stratigraphic constraints on the timing and emplacement of the Alika 2 giant Hawaiian submarine landslide, *Journal of Volcanology and Geothermal Research*, 94, 35-58

McMurtry, G. M., P. Watts, G. J. Fryer, J. R. Smith and F. Imamura (2004a), Giant landslides, mega-tsunamis, and paleo-sea level in the Hawaiian Islands, *Marine Geology*, 203,219–233, doi:10.1016/S0025-3227(03)00306-2

McMurtry, G. M., G. J. Fryer, D. R. Tappin, I. P. Wilkinson, M. Williams, J. Fietzke, D. Garbe-Schoenberg and P. Watts (2004b), Megatsunami deposits on Kohala volcano, Hawaii, from flank collapse of Mauna Loa, *Geology*, 32(9),741–744, doi: 10.1130/G20642.1

Miller, K. G., M. A. Kominz, J. V. Browning, J. D. Wright, G. S. Mountain, M. E. Katz, P. J. Sugarman, B. S. Cramer, N. Christie-Blick and S. F. Pekar (2005), The Phanerozoic Record of Global Sea-Level Change, *Science, 310*, 1293-1298, doi: 10.1126/science.1116412

Moore, J. G., D. A. Clague, R. T. Holcomb, P. W. Lipman, W. R. Normark, and M. E. Torresan (1989), Prodigious submarine landslides on the Hawaiian Ridge, *Journal of Geophysical Research: Solid Earth*, 94(B12), 17465-17484

Moore, J. G., D. A. Clague, R. T. Holcomb, P. W. Lipman, W. R. Normark and M. E. Teorresan (1992), Prodigious submarine landslides on the Hawaiian Ridge, *Journal of Geophysical Research*, 94(89), 17465-17484

Moore, J. G. and R. T. Holcomb (1994), Giant Hawaiian lantslides, *Earth and Planetary Science Letters*, 22, 119–144

Moriya, I. (2003), Toya Caldera, *In Regional geomorphology of the Japanese islands,* Edited by T. Koaze, M. Nogami, Y. Ono, and K. Hirakawa, *University of Tokyo Press,* 2, 281–288

Nakada, M. and H. Yokose (1992), Ice age as a trigger of active quaternary volcanism and tectonism, *Tectonophysics,* 212, 321-329

Oehler, J. F. (2005), Les déstabilisations de flanc des volcans de l'Ile de La Réunion. Mise en évidence, implications et origines. PhD Thesis, Univ. Blaise Pascal, Clermont-Ferrand

Oehler, J. F., J. F. Lénat and P. Labazuy (2008), Growth and collapse of the Reunion Island volcanoes, *Bulletin of Volcanology,* 70, 717–742, doi: 10.1007/s00445-007-0163-0

Ogg, J. G. (2012), Geomagnetic Polarity Time Scale. *In: The Geologic Time Scale 2012*, Edited by F. M. Gradstein, J. G. Ogg, M. D. Schmitz and G. M. Ogg, *Elsevier Publishing*, 85-114

Palmer, M. R., S. J. Hatter., T. M. Gernon., R. N. Taylor., M. Cassidy. et al (2016), Discovery of a large 2.4 Ma Plinian eruption of Basse-Terre, Guadeloupe, from the marine sediment record, *Geology*, *44*(2), 123-126

Paris, R., T. Giachetti., J. Chevalier., H. Guillou and N. Frank (2011), Tsunami deposits in Santiago Island (Cape Verde archipelago) as possible evidence of a massive flank failure of Fogos volcano, *Sedimentary Geology,* 239(3), 129-145

Paterne, M. (1980), Chronologie des éruptions ré- centes du massif de la Soufrière (Guadeloupe— Petites Antilles). Essai de comparaison des périodes d'activité volcanique de quelques grandes régions volcaniques [3rd cycle thesis]: Bordeaux, France, Université de Bordeaux, no. 1606, 165 p.

Pope. E. L., P. J. Talling, M. Urlaub, J. E. Hunt, M. A. Clare and P. Challenor, (2015), Are large submarine landslides temporally random or do uncertainties in available age constraints make it impossible to tell? *Marine Geology,* 369, 19-33

Quidelleur, X., A. Hildenbrand and A. Samper (2008), Causal link between Quaternary paleoclimatic changes and volcanic islands evolution, *Geophysical Research Letters*, *35*, 1–5, doi:10.1029/2007GL031849

Radiosonde data downloaded from http://www1.ncdc.noaa.gov/pub/data/igra/ from directory data-por/, Download file for Le Reuzet station in Guadeloupe, code GP, numeric code 78897

Ramalho, R. S., G. Winckler, J. Madeira, G. R. Helffrich, A. Hipólito, R. Quartau and J. M. Schaefer (2015), Hazard potential of volcanic flank collapses raised by new megatsunami evidence, *Science advances*, 1(9), e1500456

Reid, R.P., S. N. Carey and D. R. Ross (1996), Geological Society of America Bulletin Late Quaternary sedimentation in the Lesser Antilles island arc Late Quaternary sedimentation in the Lesser Antilles island arc, *Geological society of America Bulletin, 108*, 78-100, doi: 10.1130/0016-7606(1996)108<0078:LQSITL>2.3.CO;2

Reid, M.E. (2004), Massive collapse of volcano edifices triggered by hydrothermal pressurization, *Geology,* 32, 373-376

Samper, A., X. Quidelleur, P. Lahitte. D. Mollex (2007), Timing of effusive volcanism and collapse events within an oceanic arc island: Basse-Terre, Guadeloupe archipelago (Lesser Antilles Arc), *Earth and Planetary Science Letters, 258*, 175-191, doi:10.1016/j.epsl.2007.03.030

Samper. A., Quidelleur. X., Boudon. G., Le Friant., A., Komorowski. J. C. (2008), Radiometric dating of three large volume flank collapses in the Lesser Antilles Arc, *Journal of Volcanology and Geothermal Research*, 176, 485-492

Sato, H. P., H. Hasegawa., S. Fujiwara., M. Tobita., M. Koarai., H. Une and J. Iwahashi (2007), Interpretation of landslide distribution triggered by the 2005 Northern Pakistan earthquake using SPOT 5 imagery, *Landslides*, 4(2), 113-122

Seta, M. D. et al., (2012), Slope instability induced by volcano-tectonics as an additional source of hazard in active volcanic areas: The case of Ischia island (Italy), *Bulletin of Volcanology*, 74, 79–106

Siebert, L. (1984), Large volcanic debris avalanches: characteristics of source areas, deposits, and associated eruptions, *Journal of Volcanology and Geothermal Research*, 22, 163–197

Singer, B. S., B. R. Jicha, M. A. Harper, J. A. Naranjo, L. E. Lara and H. Moreno-Roa, (2008), Eruptive history, geochronology, and magmatic evolution of the Puyehue-Cordón Caulle volcanic complex, Chile, *Geological Society of America Bulletin, 120 (5/6)*, 599-618, doi: 10.1130/B26276.1

Soya, T., Y. Katsui, K. Niida, K. Sakai and A. Tomiya (2007), Geologic map of Usu volcano, 2nd edition, Geological Map of Volcanoes (2), Geological Survey of Japan, The National Institute of Advanced Industrial Science and Technology, Tsukuba

Stillman, C. J. (1999), Giant Miocene landslides and the evolution of Fuerteventura, Canary Islands, *Journal of Volcanological and Geothermal Research,* 94(1-4), 89–104.

Trofimovs, J. et al., (2006), Submarine pyroclastic deposits formed at the Soufrière Hills volcano, Montserrat (1995–2003): What happens when pyroclastic flows enter the ocean? *Geology*, *34(7)*, 549-552, doi: 10.1130/G22424.1

Trofimovs, J., R. S. J. Sparks and P. J. Talling (2008), Anatomy of a submarine pyroclastic flow and associated turbidity current: July 2003 dome collapse, Soufrière Hills volcano, Montserrat, West Indies, *Sedimentology*, *55*, 617-634, doi: 10.1111/j.1365-3091.2007.00914

Trofimovs, J., J. K. Fisher, H. A. MacDonald, P. J. Talling, R. S. J. Sparks, M. B. Hart, C. W. Smart, G. Boudon, C. Deplus, J. C. Komorowski, A. Le Friant, S. G. Moreton, S.G and M. J. Leg (2010), Evidence for carbonate platform failure during rapid sea-level rise; ca 14 000 year old bioclastic flow deposits in the Lesser Antilles. *Sedimentology*, *57*, 735-759, doi: 10.1111/j.1365-3091.2009.01117

Trofimovs, J., C. Foster, R. S. J. Sparks, S. Loughlin, A. Le Friant, C. Deplus, L. Porritt, T. Christopher, R. Luckett, P. J. Talling, M. R. Palmer and T. Le Bas (2012), Submarine pyroclastic deposits formed during the 20th May 2006 dome collapse of Soufrière Hills volcano, Montserrat, *Bulletin of Volcanology, 74*, 391-405, doi: 10.1007/s00445-011-0533-5

Trofimovs, J., P. J. Talling, J. K. Fisher, M. B. Hart, R. S. J. Sparks, S. F. L. Watt, M. Cassidy, C. W. Smart, A. Le Friant, S. G. Moreton and M. J. Lang (2013), Timing, origin and emplacement dynamics of mass flows offshore of SE Montserrat in the last 110 ka: Implications for landslide and tsunami hazards, eruption history, and volcanic island evolution, *Geochemistry, Geophysics, Geosystems*, *14(2)*, 385–406. doi:10.1002/ggge.20052

Urgeles, R., M. Canals, J. Baraza and B. Alonso (1997), The most recent megalandslides of the Canary Islands: El Golfo debris avalanche and Canary debris flow, west El Hierro Island, *Journal of Geophysical Resarch*, 102, 20305-20323

Urgeles, R., D. G. Masson, M. Canals, A. B. Watts and T. Le Bas (1999), Recurrent large-scale landsliding of the west flank of La Palma, Canary Islands, *Journal of Geophysical Research*, 104 (B11), 25331-25348, doi: 1999JB900243 0148-0227/99/1999JB 900243$09.00

Vezzoli, L., (1988), Island of Ischia, *CNR Quaderni de La ricerca scientifica*, 114(10), 122

Vincent, P. M., J. L. Bourdier, G. Boudon (1989), The primitive volcano of Mount Pelée: its construction and partial destruction by flank collapse, *Journal of volcanology and geothermal research*, 38(1), 1-15

Wadge, G. (1985), Morne Patates volcano, Southern Dominica, Lesser Antilles, *Geological Magazine*, *122 (3)*, 253–260

Wadge. G., B. Voight, R. S. J. Sparks, P. D. Cole, S. C. Loughlin, and R. E. A. Robertson (2014), An overview of the eruption of Soufrière Hills Volcano, Montserrat from 2000 to 2010, *in The Eruption of the Soufrière Hills Volcano, Montserrat from 2000–2010, Memoirs of the Geological Society of London 3*, edited by G. Wadge, R. A. E.Robertson, and B. Voight, *Geological Society of London,*1–4

Wall-Palmer, D., et al., (2014), Late Pleistocene stratigraphy of IODP Site U1396 and compiled chronology offshore of south and south west Montserrat, Lesser Antilles, *Geochemistry, Geophysics, Geosystems*, *15*, 1–21, doi: 10.1002/2014GC005402/full

Ward, S. N. and S. Day (2003), Ritter Island Volcano-lateral collapse and the tsunami of 1888, *Geophysical Journal International, 154*, 891-902

Watt, S. F. L., et al., (2012a), Combinations of volcanic-flank and seafloor-sediment failure offshore Montserrat, and their implications for tsunami generation, *Earth and Planetary Science Letters*, *319(320)*, 228–240, doi:10.1016/j.epsl.2011.11.032

Watt, S. F. L., et al., (2012b), Widespread and progressive seafloor-sediment failure following volcanic debris avalanche emplacement: Landslide dynamics and timing offshore Montserrat, Lesser Antilles, *Marine Geology*, *323(325)*, 69–94, http://dx.doi.org/10.1016/j.margeo.2012.08.002

Watt, S. F. L., P. J. Talling and J. E. Hunt (2014), New insights into the emplacement dynamics of volcanic island landslides, *Oceanography,* 27, 46–57

Weaver, P. P. E., R. G. Rothwell, J. Ebbing, D, Gunn and P. M. Hunter (1992), Correlation, frequency of emplacement and source directions of megaturbidites on the Madeira Abyssal Plain, *Marine Geology*, 109(1-2), 1-20

Figure 1. Topographic and bathymetric map of Montserrat showing site of U1395B and large debris avalanche flows [Le Friant et al., 2004; Boudon et al., 2007; Lebas et al., 2011; Watt et al., 2012a, 2012b] .

Figure 2: Upper 44 m of Hole U1395B including core log and photos; calculated sedimentation rates for all age models; NRM declination data from shipboard measurements; section of stratigraphic core photos and log; sample of componentry data; oxygen isotopes from this study and the global oxygen isotope curve from Lisiecki and

Raymo [2005]. For full componentry data and stratigraphic log of Hole U1395B see supplementary data.

Figure 3: Correlations of the top of core U1395B with shallow cores based on componentry and oxygen isotope data [Le Friant et al., 2008; Cassidy et al., 2012b, 2013; Ogg et al., 2012; Trofimovs et al., 2013; Wall-Palmer et al., 2014].

Figure 4: Timing of (a) all events, (b) volcaniclastic events (tephra fall and turbidite deposits; including mixed composition turbidites), (c) volcaniclastic events (tephra fall and volcaniclastic turbidite), (d) tephra fall deposits, and (e) all turbidites at Montserrat. In each case, three different age models are shown. Age model 1 (green) uses oxygen isotope data, biostratigraphic data, AMS dates, and paleomagnetic dates. Age model 2 (red) uses Deposit 2 as a boundary at 130 ka (Figure 2), and the paleomagnetic intervals. Age model 3 (blue) uses only the paleomagnetic data. Clustering of events in all age models can be seen at ~950-860 ka, 810-750 ka, 200-100 ka and from ~50 ka, on Montserrat. There is an absence of prolonged pauses in activity. Thin grey lines show occurrence of scoria within core U1395B, the thick grey line shows known extents of activity at volcanic centres on Montserrat based on limited subaerial dating [Harford et al., 2002].

Figure 5: Number of events within 50 kyr (centred on window, at 10 kyr increments). Peaks correspond to clusters in Figure 4. Age model 1 (green) uses oxygen isotope data, biostratigraphic data, AMS dates, and paleomagnetic dates. Age model 2 (red) uses Deposit 2 as a boundary at 130 ka (Figure 2), and the paleomagnetic intervals. Age model 3 (blue) uses only the paleomagnetic data. Peaks in event frequency occur at ~930 ka to

~900 ka, ~810 ka to ~760 ka, and ~190 ka to ~120 ka. Periods when event frequency is above the 90% confidence interval in all age models are shaded in grey. The black line is the Miller et al., [2005] sea-level curve in meters from present day sea-level. Thin grey lines show occurrence of mafic scoria within Hole U1395B, the thick grey line shows known extents of activity at volcanic centres on Montserrat based on limited subaerial dating [Harford et al., 2002]. There is a peak in event frequency that coincides with the appearance of mafic scoria in Hole U1395B and all large flank collapses occur during periods of rapid sea-level rise.

Figure 6: A. Diagram summarising the age of large (>0.3 km^3) landslides around volcanic islands and sea-level. The sea-level curve used is Miller et al., [2005]. Events considered have date errors of <±22.5 ka. Periods of rapid sea-level rise (>5m/ka) are highlighted in blue. Vertical bars show errors of individual landslide ages. Ocean island landslides are shown in green, and island arc landslides are shown in red. Letters identify indiviual landslides and correspond to letters in Table 3. B. Comparison of sea level conditions with those at the time of documented landslides (Table 3) using data in 5 ka bins. Grey solid circles indicate the full range of conditions over the past 1 Ma at which no landslides were recorded. Annotated box and whisker plots indicate the spread of each data set, with boxes showing 25%, 50% and 75% of the data, whiskers showing the minimum and maximum. Numbers next to data points show the number of overlapping datum. A general skew of landslides occurring at rapid sea-level rises can be seen in the box and whisker plots.

Allocation number	Publication code	Sample identifier	$\delta^{13}C_{VPDB}$‰ ± 0.1	Carbon content (% by wt.)	^{14}C Enrichment (% modern)	+/- 1σ (% modern)	Conventional Radiocarbon Age (years BP)	+/- 1σ (radiocarbon yrs BP)	Stratigraphic position (cm)
1721.0513	SUERC-46961	1H2W-108-110	1.1	10.9	28.82	0.13	9993	37	258-260
1721.0513	SUERC-46962	1H2W-115-117	1.1	10.8	23.93	0.12	11489	40	265-267
1721.0513	SUERC-46965	1H3W-109-111	1.2	11.4	0.33	0.06	45806	1463	409-411
1721.0513	SUERC-46966	1H3W-116-118	1.0	11.3	0.40	0.06	44294	1208	416-418

Table 1: AMS carbon dates from core U1395.

	Age Model 1	**Age Model 2**	**Age Model 3**
Linear model	0.0898	*0.00176*	*0.00285*
Generalised linear model	0.083407	*0.00138*	*0.00696*
Proportional hazards model	0.106	*0.00219*	*0.00942*

Table 2: Results of linear statistical tests for turbidite frequency and sea-level correlations. Italicised values show when statistical tests are significant, (ie when the null hypothesis can be rejected).

Table 3: Global landslide database for ocean island landslides and island arc landslides with volumes >0.3 km^3 and with age errors of $< \pm 22.5$ kyr.

Flank collapse name	Country/ Island	Age (ka)	Volume (km^3)	References	Letter in Supplement -ary Figure S4
		Ocean Islands			
El Golfo	Canary Islands, El Heirro	20-10	150	Weaver et al., [1992]; Longpre et al., [2011]; Hunt et al., [2013]	a
El Julan	Canary Islands, El Heirro	550-530	130	Hunt et al., [2013]	b
Cumbre Nueva	Canary Islands, La Palma	574-529	95	Costa et al. [2014]	c
Icod	Canary Islands, Tenerife	170-160	320	Ancochea et al., [1990]; Wynn et al., [2002]; Carraceado et al., [2007]; Hunt et al., [2013, 2014]	d
Orotava	Canary Islands, Tenerife	566-525	1000	Watts and Masson [1995]; Masson et al., [2002]; Boulestreix et al., [2013]; Hunt et al., [2013]	e
Guimar	Canary Islands, Tenerife	860-840	120	Krastel et al., [2001]	f
Fogo	Cape Verde	80-66	160	Ramalho et al., [2015]	g
Alika 2	Hawaii, Mauna Loa	132-122	>0.5	McMurty et al. [1999]	h
Tahiti North	Tahitian Archipelago, Tahiti	870-850	800	Clouard et al., [2000]; Hildenbrand et al., [2004, 2006].	i
		Island Arcs			
Carmichaël	Lesser Antilles, Guadeloupe	11.5-6.9	0.3	Boudo et al., [1984, 2007]	j
Carbet	Lesser Antilles, Guadeloupe	3.5-2.8	0.5	Boudon et al., [1984, 2007]; Jerime [1979]; Paterne [1980]; Daigun [1981]; Daigun et al., [1981]	k
La Soufriere	Lesser Antilles, Dominica	6.7-2.3	6 to 7	Le Friant et al., [2002]; Boudon et al., [2007]	l
South	Italy, Ischia	3-2.4	1.5	de Alteriis et al., [2010, 2014]	m
Piettre Rosse	Italy, Ischia	40-2.4	>0.3	Vezzoli [1988]; Buchner [1986]; Seta et al., [2012]	n
Falanga	Italy, Ischia	2.4	>0.3	Buchner [1986]; Seta et al., [2012]	o
Casamicciola (NDDe)	Italy, Ischia	2.8	>0.3	de Vita et al., [2010]; Seta et al., [2012]	p
NDDw	Italy, Ischia	<10 ka		Vezzoli et al., [1988]; de Aleriis and Violante, [2009]; Seta et al., [2012]	q
D1	Lesser Antilles Martinique	129-124	>25	Germa et al., [2011]	r
D2 or the St Pierre event	Lesser Antiiles, Martinique	23.6-26.4	13	Vincent et al., [1989]; Le Friant et al., [2003]	s
D3 or Rivière Sèche event	Lesser Antiiles, Martinique	9.8-8	2	Le Friant et al., [2003]; Boudon et al., [2007]	t
Usu	Japan, Hokkaido	8-7	1 to 2	Moriya, [2003] (in Japanese); Soya et al., [2007]; Yoshida et al., [2012]	u
Ritter	Papua New Guinea, Ritter Island	0.1	5	Cooke [1981]; Ward and Day [2003]	v
Deposit 1	Lesser Antilles, Montserrat	14-11	1.8	Trofimovs et al. [2013]; Watt et al. [2012a], [2012b]; Le Friant et al. [2004]; Lebas et al. [2011]	w
Deposit 2	Lesser Antilles, Montserrat	146-112	9	Harford et al. [2002]; Le Friant et al. [2004]; Lebas et al. [2011]; Watt et al. [2012a], [2012b]; Crutchley et al. [2013]	x
Deposit 5	Lesser Antilles, Montserrat	12-8	0.3	Cassidy et al. [2013]; Le Friant et al. [2004]; Lebas et al. [2011]	y

Figure 1

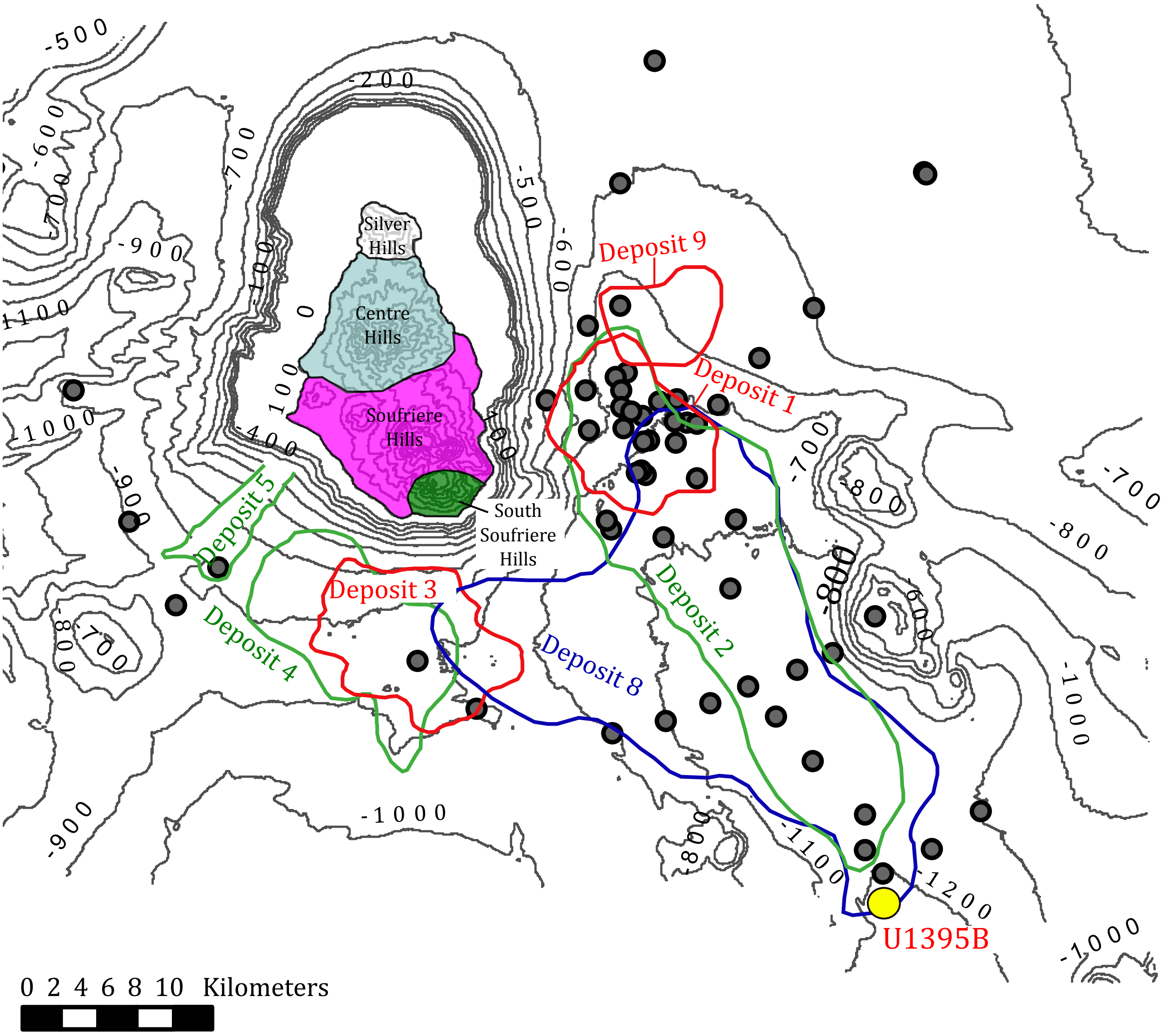

KEY

contours every 100 m above sea level

large flank collapse deposit outline (near surface)

large flank collapse deposit outline (buried)

large flank collapse deposit outline (deeply buried)

shallow vibrocore locations (Trofimovs et al., 2013)

site of IODP core U1395B

Figure 2

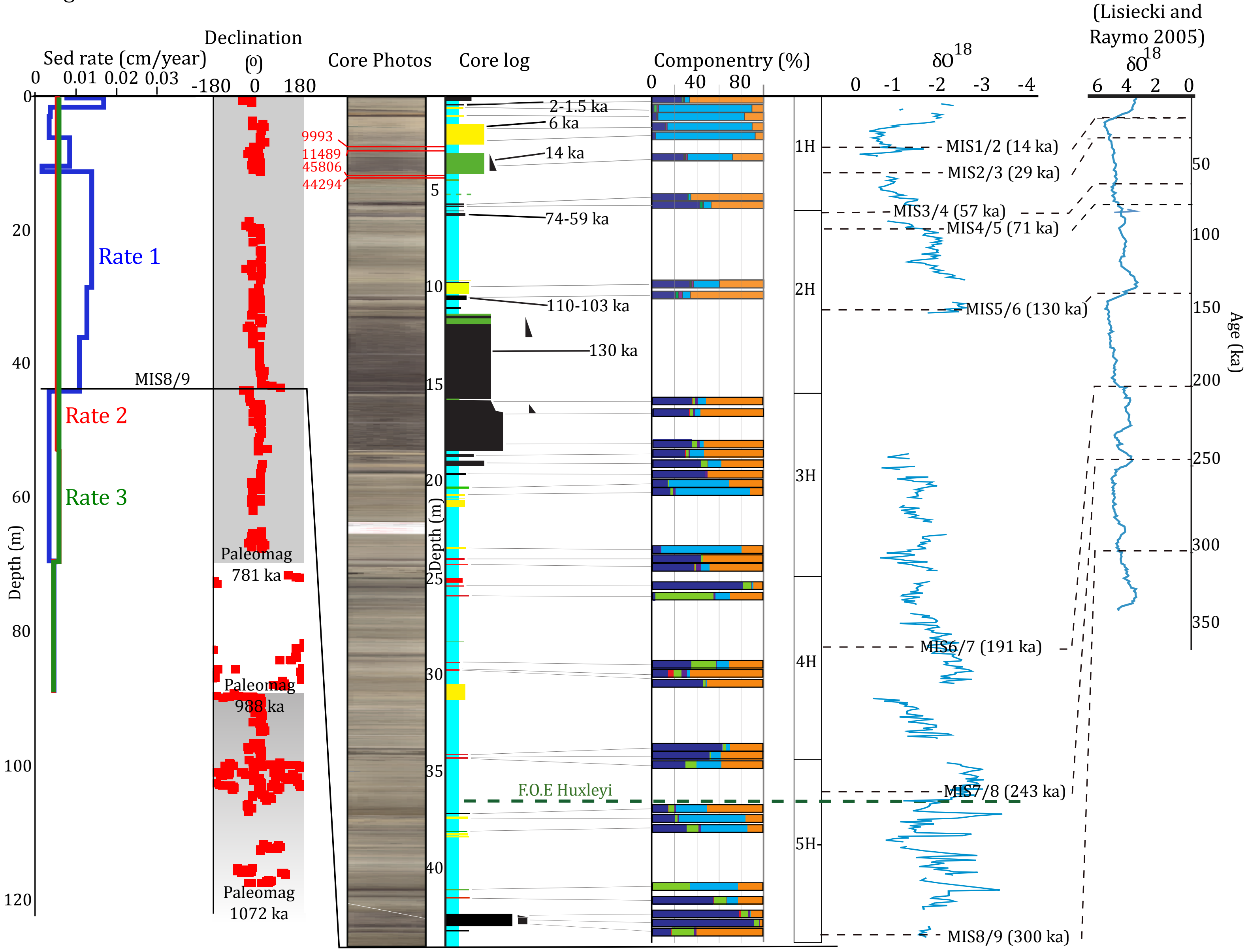

KEY

Stratigraphic log
- hemipelagic mud
- bioclastic turbidites (>70% Bioclasts
- mixed turbidites (30-70% Bioclasts)
- volcaniclastic turbidies (<30% bioclasts, Folk and Ward sorting coefficient >0.5)
- tephra (<30% bioclasts, Folk and Ward sorting coefficient <0.5)

Componentry
- glass and crystal
- bioclast
- altered lithic
- mafic
- dense andesite
- andesitic pumice

Other
- first occurence (F. O) of E. Huxleyi
- 9993 AMS radiocarbon dates (in uncalibrated years)
- Grading
- 74-59 kyr units correlated with vibrocores (Trofimovs et al. 2013)
- sedimentation rates, age model 1
- sedimentation rates, age model 2
- sedimentation rates, age model 3

Figure 3

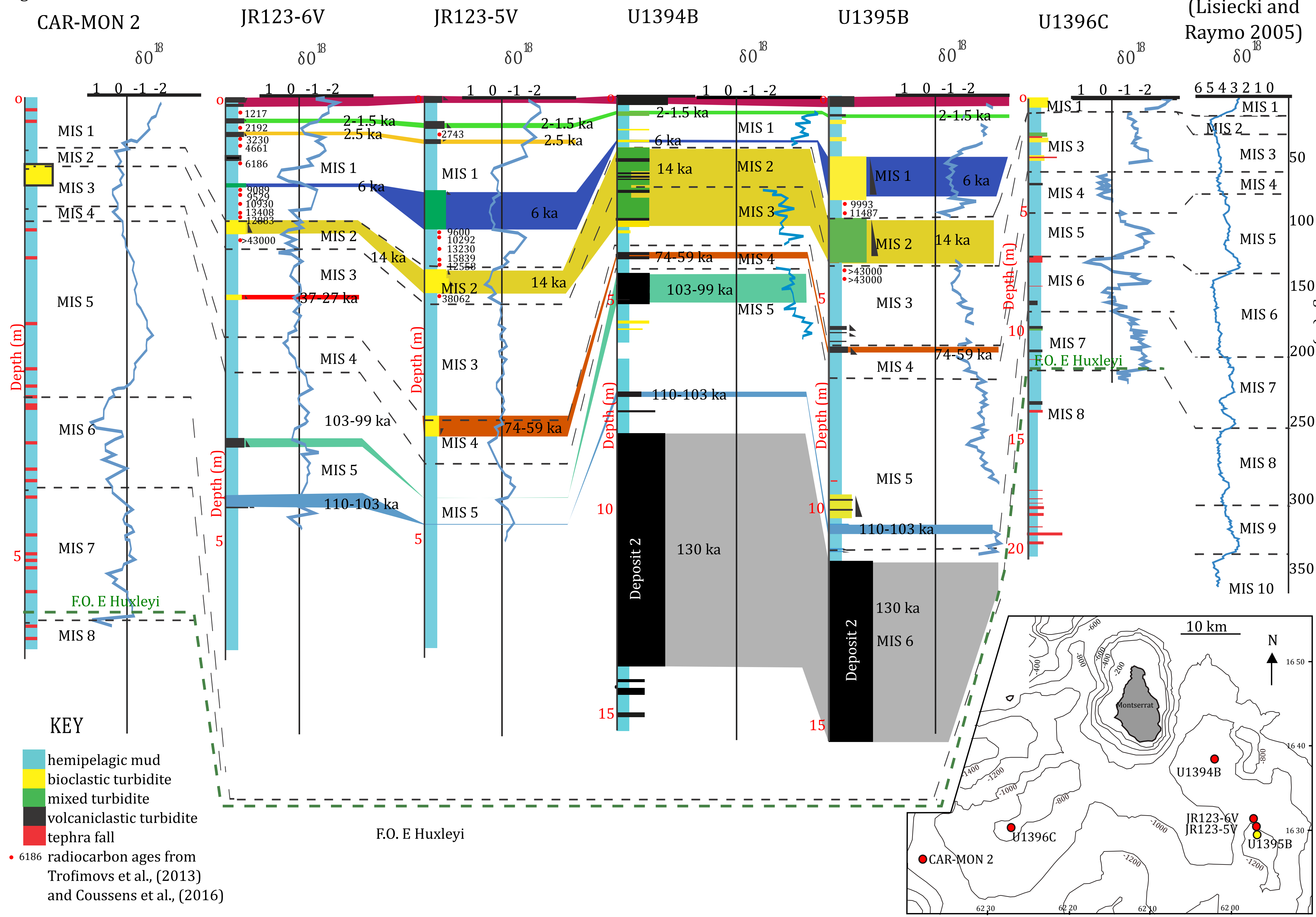

CAR-MON 2
JR123-6V
JR123-5V
U1394B
U1395B
U1396C
Global (Lisiecki and Raymo 2005)
δ0 18
Depth (m)
Age (ka)
MIS 1
MIS 2
MIS 3
MIS 4
MIS 5
MIS 6
MIS 7
MIS 8
MIS 9
MIS 10
F.O. E Huxleyi
2-1.5 ka
2.5 ka
6 ka
14 ka
37-27 ka
74-59 ka
103-99 ka
110-103 ka
130 ka
Deposit 2
10 km
N
Montserrat
U1394B
JR123-6V
JR123-5V
U1395B
U1396C
CAR-MON 2
KEY
hemipelagic mud
bioclastic turbidite
mixed turbidite
volcaniclastic turbidite
tephra fall
6186 radiocarbon ages from Trofimovs et al., (2013) and Coussens et al., (2016)
F.O. E Huxleyi

Figure 4

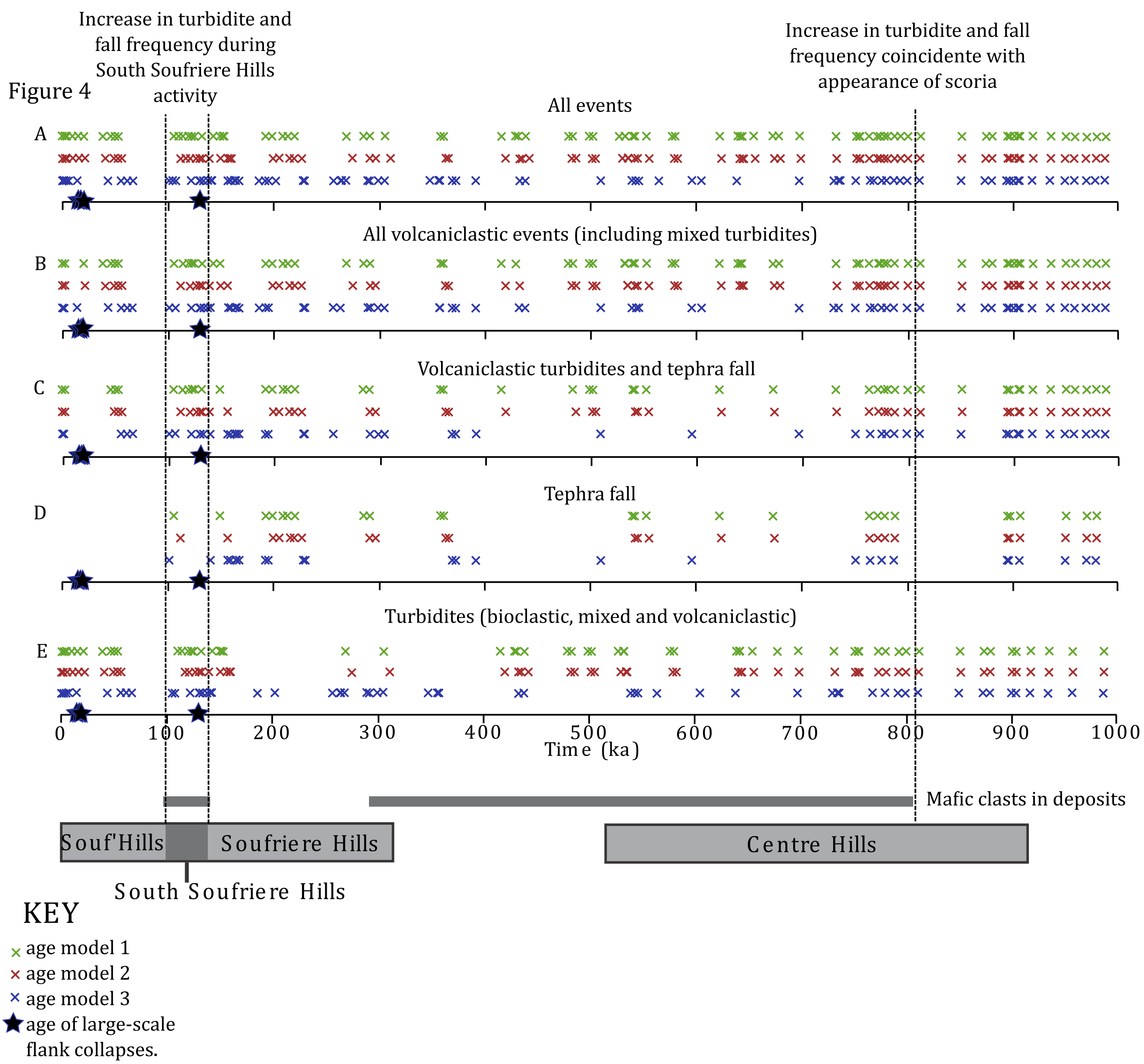

Increase in turbidite and fall frequency during South Soufriere Hills activity
Increase in turbidite and fall frequency coincidente with appearance of scoria
All events
A
All volcaniclastic events (including mixed turbidites)
B
Volcaniclastic turbidites and tephra fall
C
Tephra fall
D
Turbidites (bioclastic, mixed and volcaniclastic)
E
0
100
200
300
400
500
600
700
800
900
1000
Time (ka)
Mafic clasts in deposits
Souf'Hills
Soufriere Hills
Centre Hills
South Soufriere Hills
KEY
age model 1
age model 2
age model 3
age of large-scale flank collapses.

Figure 5

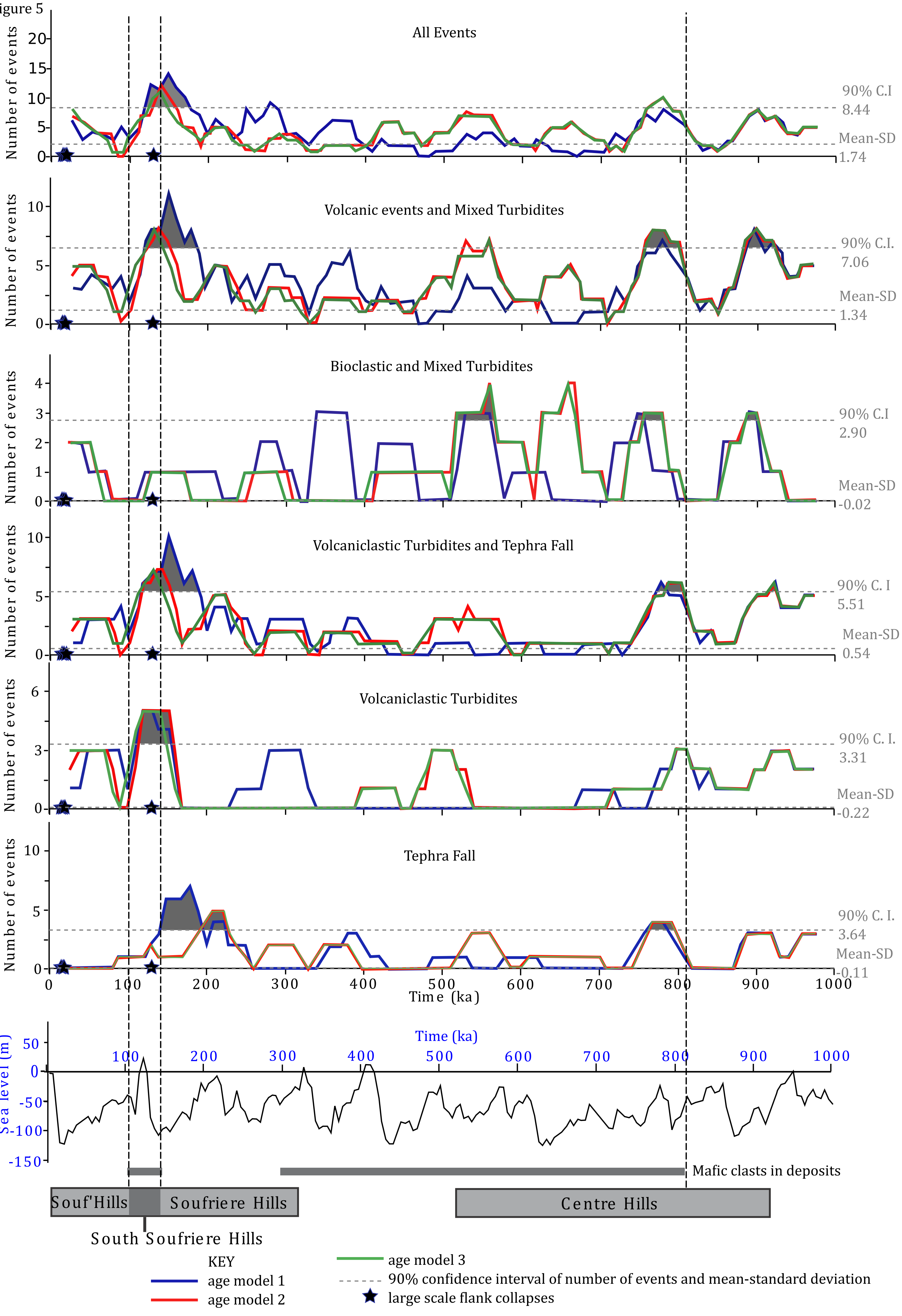

All Events
Number of events
90% C.I
8.44
Mean-SD
1.74
Volcanic events and Mixed Turbidites
90% C.I.
7.06
Mean-SD
1.34
Bioclastic and Mixed Turbidites
90% C.I
2.90
Mean-SD
-0.02
Volcaniclastic Turbidites and Tephra Fall
90% C. I
5.51
Mean-SD
0.54
Volcaniclastic Turbidites
90% C. I.
3.31
Mean-SD
-0.22
Tephra Fall
90% C. I.
3.64
Mean-SD
-0.11
Time (ka)
Sea level (m)
Time (ka)
Mafic clasts in deposits
Souf'Hills
Soufriere Hills
Centre Hills
South Soufriere Hills
KEY
age model 1
age model 2
age model 3
90% confidence interval of number of events and mean-standard deviation
large scale flank collapses

Figure 6

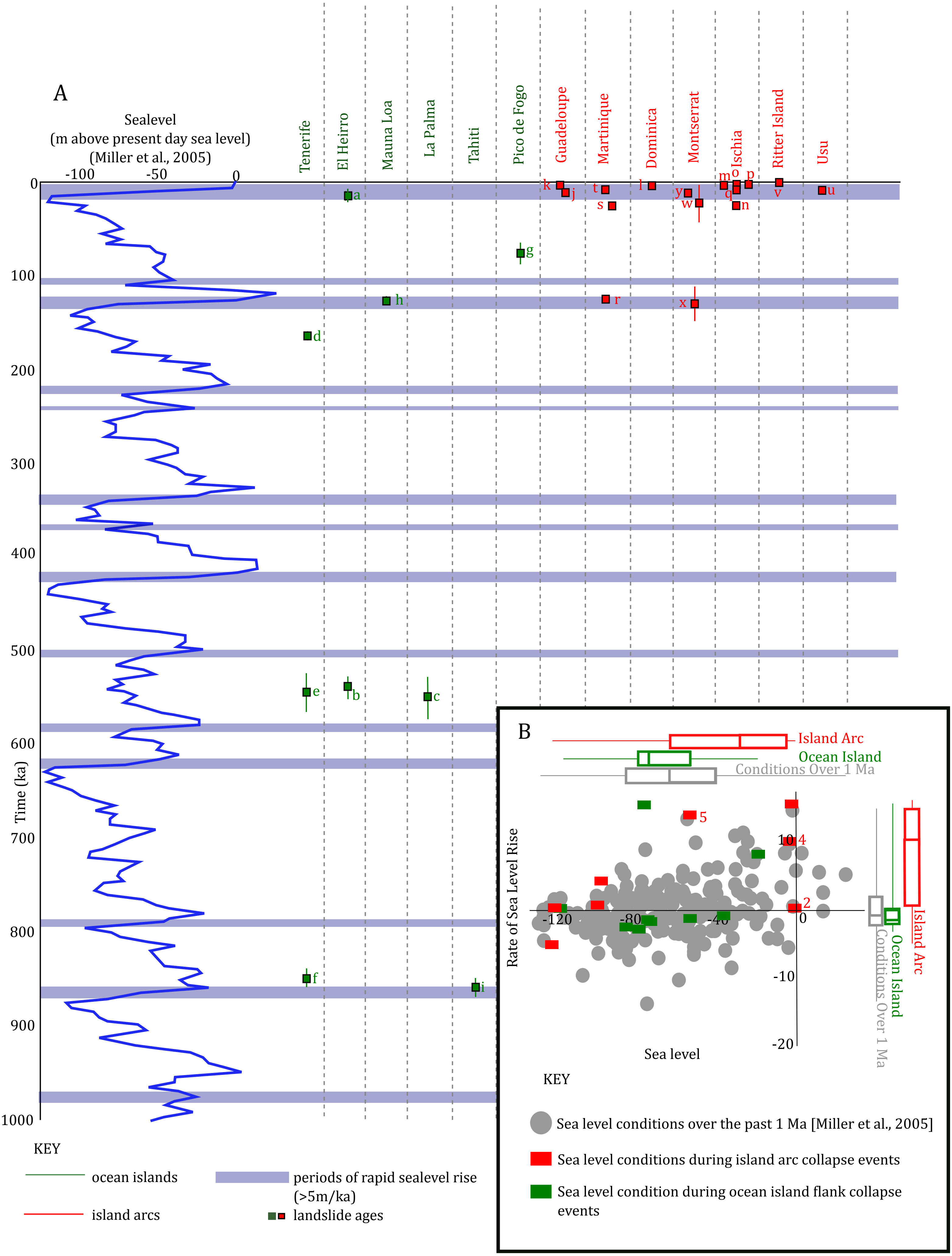
A
Sealevel
(m above present day sea level)
(Miller et al., 2005)
-100
-50
0
Tenerife
El Heirro
Mauna Loa
La Palma
Tahiti
Pico de Fogo
Guadeloupe
Martinique
Dominica
Montserrat
Ischia
Ritter Island
Usu
Time (ka)
0
100
200
300
400
500
600
700
800
900
1000
B
Island Arc
Ocean Island
Conditions Over 1 Ma
Rate of Sea Level Rise
Sea level
-120
-80
-40
0
10
-10
-20
KEY
Sea level conditions over the past 1 Ma [Miller et al., 2005]
Sea level conditions during island arc collapse events
Sea level condition during ocean island flank collapse events
KEY
ocean islands
island arcs
periods of rapid sealevel rise (>5m/ka)
landslide ages